

(12)

AFGL-TR-85-0064

PROJECT ABLE: ATMOSPHERIC BALLOONBORNE
LIDAR EXPERIMENT

O. Shepherd
G. Aurilio
R.D. Bucknam
A.G. Hurd
W.H. Sheehan

20000801152

AD-A160 372

Visidyne, Inc.
5 Corporate Place
South Bedford Street
Burlington, MA 01803

25 March 1985

Final Report
22 September 1981 through 22 February 1985

DTIC FILE COPY

Approved for public release; distribution unlimited

AIR FORCE GEOPHYSICS LABORATORY
AIR FORCE SYSTEMS COMMAND
UNITED STATES AIR FORCE
HANSCOM AFB, MASSACHUSETTS 01731

DTIC
ELECTE
OCT 16 1985
S D
B

Reproduced From
Best Available Copy

85 10 16 111

This technical report has been reviewed and is approved for publication.

Robert W. Fenner

DONALD E. BEDO
Contract Manager

Robert W. Fenner

ROBERT W. FENNER
Branch Chief

FOR THE COMMANDER

John S. Garing

JOHN S. GARING
Division Director

This report has been reviewed by the ESD Public Affairs Office (PA) and is releasable to the National Technical Information Service (NTIS).

Qualified requestors may obtain additional copies from the Defense Technical Information Center. All others should apply to the National Technical Information Service.

If your address has changed, or if you wish to be removed from the mailing list, or if the addressee is no longer employed by your organization, please notify APGL/DAA, Hanscom AFB, MA 01731. This will assist us in maintaining a current mailing list.

UNCLASSIFIED

SECURITY CLASSIFICATION OF THIS PAGE

REPORT DOCUMENTATION PAGE

1a. REPORT SECURITY CLASSIFICATION Unclassified		1b. RESTRICTIVE MARKINGS	
2a. SECURITY CLASSIFICATION AUTHORITY		3. DISTRIBUTION/AVAILABILITY OF REPORT Approved for public release; Distribution unlimited.	
2b. DECLASSIFICATION/DOWNGRADING SCHEDULE			
4. PERFORMING ORGANIZATION REPORT NUMBER(S) VI-824		5. MONITORING ORGANIZATION REPORT NUMBER(S) AFGL-TR-85-0064	
6a. NAME OF PERFORMING ORGANIZATION Visidyne, Inc.	6b. OFFICE SYMBOL (If applicable)	7a. NAME OF MONITORING ORGANIZATION Air Force Geophysics Laboratory	
6c. ADDRESS (City, State and ZIP Code) 5 Corporate Place, S. Bedford Street Burlington, MA. 01803		7b. ADDRESS (City, State and ZIP Code) Hanscom AFB, Massachusetts 01731 Monitor: Donald E. Bedo/OPA	
8a. NAME OF FUNDING SPONSORING ORGANIZATION	8b. OFFICE SYMBOL (If applicable)	9. PROCUREMENT INSTRUMENT IDENTIFICATION NUMBER F19628-81-C-0165	
3c. ADDRESS (City, State and ZIP Code)		10. SOURCE OF FUNDING NCS.	
		PROGRAM ELEMENT NO. 62101F	PROJECT NO. 6690
		TASK NO. 04	WORK UNIT NO. AL
11. TITLE (Include Security Classification) Project ABLE: Atmospheric Balloonborne Lidar Experiment (U)			
12. PERSONAL AUTHOR(S) O. Shepherd, G. Aurilio, R.D. Bucknam, A.G. Hurd, W.H. Sheehan			
13a. TYPE OF REPORT Final Report	13b. TIME COVERED FROM 22SEP81 TO 22FEB85	14. DATE OF REPORT (Yr., Mo., Day) 1985 March 25	15. PAGE COUNT 96
16. SUPPLEMENTARY NOTATION			
17. COSATI CODES		18. SUBJECT TERMS (Continue on reverse if necessary and identify by block number)	
FIELD	GROUP	SUB. GR.	Lidar; Balloonborne Payload; Atmospheric Density;
			Neodymium:YAG Laser; Rayleigh Scattering; Aerosol Scattering;
19. ABSTRACT (Continue on reverse if necessary and identify by block number) The object of this contract was to fabricate and operate in a field test a balloonborne lidar experiment capable of performing nighttime atmospheric density measurements up to 70 km altitude with a resolution of 150 meters. The payload included a frequency-doubled and -tripled Nd:YAG laser with outputs at 355 and 532 nm, a telescoped receiver with PMT detectors, a command-controlled optical pointing system, and support systems, including thermal control, telemetry, command, and power. Successful backscatter measurements were made during field operations which included a balloon launch from Roswell, New Mexico and a flight over the White Sands Missile Range.			
20. DISTRIBUTION/AVAILABILITY OF ABSTRACT UNCLASSIFIED/UNLIMITED <input type="checkbox"/> SAME AS RPT. <input type="checkbox"/> DTIC USERS <input type="checkbox"/>		21. ABSTRACT SECURITY CLASSIFICATION Unclassified	
22a. NAME OF RESPONSIBLE INDIVIDUAL Donald E. Bedo		22b. TELEPHONE NUMBER (Include Area Code) (617) 861-3661	22c. OFFICE SYMBOL OPA

DD FORM 1473, 83 APR

EDITION OF 1 JAN 73 IS OBSOLETE.

Unclassified
SECURITY CLASSIFICATION OF THIS PAGE

TABLE OF CONTENTS

TITLE	PAGE
Preface	7
1. Introduction	9
2. Experiment Description	10
3. System Design	15
3.1 Payload Structure	17
3.2 Transmitter	21
3.2.1 Laser	21
3.2.2 Laser Energy Monitor	25
3.2.3 Transmitter System	27
3.3 Receiver	27
3.3.1 Telescope Assembly	31
3.3.2 Beam Splitter and Filter Assembly	33
3.3.3 Detector Assemblies	33
3.4 Optical Pointing System	36
3.5 Thermal Control System	36
3.6 Payload Electronics	41
3.6.1 Payload Power	41
3.6.2 Telemetry	41
3.6.3 Payload Orientation System	44
3.7 Data and Command Software	45
4. Safety Considerations	45
4.1 Introduction	45
4.2 Laboratory Safety	45
4.3 Range Safety Requirements	46
5. Test, Calibration, and Alignment	48
5.1 Transmitter Tests	48
5.2 Receiver Tests	48
5.3 Pointing System Tests	48
5.4 Thermal Control System Tests	49
5.5 System Testing	49
5.5.1 Optical Alignment	49
5.5.2 Lidar Calibration	51
5.6 Environmental Tests	51
5.6.1 Pressure Vessel Test	53
5.6.2 Shock Test	53
5.6.3 Thermovac Test	53
6. Field Operations	55
6.1 Scenario	55
6.2 Thermovac Test	57
6.2.1 Test Setup and Procedures	57
6.2.2 Test Results	57

TABLE OF CONTENTS

TITLE	PAGE
7. Flight Operations	62
7.1 System Tests	62
7.2 Flight Summary	66
7.2.1 Laser	66
7.2.2 Laser Energy Monitor (LEM)	67
7.2.3 Receiver	67
7.2.4 Data and Command	67
7.2.5 Thermal Control	68
7.2.6 Payload	68
7.3 Payload Recovery	68
7.4 Quick-look Data	68
8. Recommendations and Conclusions	71
8.1 Frame	71
8.2 Laser Refurbishment	71
8.3 Harmonic Generator Encoder	71
8.4 Thermal Control System Modification	71
8.5 Laser Signal Detector	71
8.6 1064 nm Detector	71
8.7 Summary	71
9. References	73
APPENDIX A Report on Lidar Balloon Gondola Frame Analysis	75
APPENDIX B ABLE Laser Test Summary	79
APPENDIX C Pre-flight Briefing/ABLE	81
APPENDIX D Flight Control Personnel and Work Station	83
APPENDIX E Launch Schedule	85
APPENDIX F Project ABLE Launch Countdown	87
APPENDIX G Instrumentation Checks	89
APPENDIX H Pre-flight Check List	91
APPENDIX I Pre-Rollout Check	93
APPENDIX J ABLE Flight Operations	95

Accession For	
NTIS GRA&I	<input checked="" type="checkbox"/>
DTIC TAB	<input type="checkbox"/>
Unannounced	<input type="checkbox"/>
Justification	
By	
Distribution/	
Availability Codes	
Dist	Avail and/or Special
A-1	



LIST OF ILLUSTRATIONS

<u>FIGURE</u>		<u>PAGE</u>
1.	ABLE Payload on Day of Launch	11
2.	Predicted Signal Level Calculation Geometry	12
3.	Balloon Launch Preparation.	14
4.	ABLE Payload during Final Assembly, Forward View.	18
5.	ABLE Payload during Final Assembly, Aft View.	19
6.	ABLE Payload, Quarter-scale Model	20
7.	Nd:YAG Laser prior to Payload Assembly.	22
8.	Laser Optical Layout.	23
9.	Laser Energy Monitor (LEM) Details.	26
10.	Laser Mounted in Payload Pressure Chamber	28
11.	Receiver Optics Layout.	29
12.	Detector Electronics, Simplified Schematic.	35
13.	Pointing Mirror System.	37
14.	Lidar Cooling System.	39
15.	ABLE Payload Electronics, Block Diagram	42
16.	Lidar Detector Data Flow.	43
17.	Optical Alignment Methods	50
18.	Optical Axis Alignment System	52
19.	Site of ABLE 1984 Field Operations.	56
20.	ABLE Payload Set Up for Thermovac Test.	59
21.	Thermovac Chamber Altitude and Temperature during ABLE Payload Test.	61
22.	Laser/LEM Calibration Test.	63
23.	ABLE Payload and Balloon Prior to Launch.	65
24.	ABLE Payload at Recovery Site	69
25.	Quick-look Data Sample.	70

LIST OF TABLES

TABLE

PAGE

1.	Balloonborne Lidar Specifications	16
2.	Project ABLE Laser Specifications	24
3.	Lidar Receiver Optical Specifications	30
4.	Dall-Kirkham Optical System Data.	32
5.	Detector Specifications	34
6.	Lidar Cooling System.	40
7.	Payload Environmental Specifications.	54
8.	ABLE Launch Schedule - 1984	58
9.	Stratosphere Chamber Specifications	60

PREFACE

The authors wish to acknowledge the extensive program support provided by Drs. J. W. Carpenter and W. P. Reidy and the technical contributions of R. W. Brooke, Dr. R. D. Wattson, and T. F. Zehnpfennig of Visidyne's staff which were an important part of the ultimate success of the ABLE experiment.

We also appreciate the close cooperative efforts of AFGL personnel, in particular Dr. D. E. Bedo and R. A. Swirbalus, and wish to commend A. Griffin and other AFGL/LC personnel for their successful launch operations.

THIS PAGE LEFT BLANK INTENTIONALLY

1. INTRODUCTION

Project ABLE (Atmospheric Balloon Lidar Experiment) is part of Air Force ^{The A.F.} Geophysics Laboratory's continuing interest in developing techniques for making remote measurements of atmospheric quantities such as density, pressure, temperatures, and wind motions. The system consists of a balloonborne lidar payload designed to measure neutral molecular density as a function of altitude from ground level to 70 km. The lidar provides backscatter data at the doubled and tripled frequencies of a Nd:YAG laser, which will assist in the separation of the molecular and aerosol contributions and subsequent determination of molecular density vs altitude. → (10/8/72)

Previous work on the proposed experiment was performed by General Electric Space Division in a feasibility study^[1] and by Visidyne, Inc. in a design study.^[2] The development performed under the present contract is a precursor for future space lidar systems.

The experiment development included the following:

1. Laboratory testing of the flight laser
2. Mechanical design, fabrication, and test of the lidar receiver, pressure chambers, assorted optical mounts, and payload structure
3. Optical design, assembly, and test of the receiver telescope, receiver optics, and lidar alignment devices
4. Electrical design, fabrication, and test of the payload power distribution system, data system, uplink command systems, and housekeeping system
5. Design, fabrication, and test of the payload thermal control and monitoring system
6. Design, development, test, and installation of the onboard software/firmware required to support the data and command systems
7. Design, development, and test of a payload ground support system
8. Development and implementation of component, subsystems, and lidar system test and calibration procedures.
9. Integration of the payload with the balloon system
10. Preparation of a launch scenario and schedule
11. Planning and performing the all-up test in the Holloman AFB thermovac chamber
12. Field testing and launch support for the successful ABLE flight

13. Support for the post-flight payload recovery operation
14. Performance of a post-flight engineering evaluation of the experiment performance.

Documentation previously submitted by Visidyne as a part of the contractual requirements includes quarterly R and D status reports, R and D Design Evaluation Report, R and D Test and Acceptance Plan, R and D Equipment Information Report, and ABLE Interface Control Document.

On August 23, 1984 at 2130 hr local time, the ABLE, payload shown in Figure 1, was launched from Roswell, New Mexico. The payload attained an altitude of 107,000 ft approximately 3 hours after launch. The lidar experiment was operated successfully at altitudes greater than 60,000 ft as per the experiment plan. The objectives of the flight were to provide an experiment test of a balloonborne lidar and to make atmospheric backscatter measurements with 150 meter slant range resolution using a lidar system. Both objectives were met.

The ABLE payload is a complete system incorporating a variety of high technology devices and operations. Nevertheless, its development and flight operation met all technical objectives, it was completed on schedule, and it was within the prescribed budget. This was a major accomplishment for the first flight of a prototype payload.

2. EXPERIMENT DESCRIPTION

The principal objective of the present ABLE experiment was to design, fabricate, and deploy a balloonborne lidar system to measure neutral atmospheric molecular density as a function of altitude from ground level to 70 km.

The basic scattering geometry of the ABLE experiment system for measurements of atmospheric density is shown in Figure 2. The balloon floats at an altitude h_0 as laser pulses are fired into the atmosphere at a zenith angle θ . The laser pulse propagates through the atmosphere, and in each volume element, $\delta V = \alpha_L D^2 \delta D$, a small fraction of the photons are Rayleigh scattered by air molecules or suffer other scatterings and absorptions due to aerosols and other constituents. For each laser pulse, the number of photons from δV that are Rayleigh backscattered into the collecting mirror on the balloon payload is given by

$$N_\lambda = \frac{c_\lambda}{h\nu} f_{\sigma_\lambda} N(z) \delta D \frac{A}{4\pi D^2} T_\lambda$$

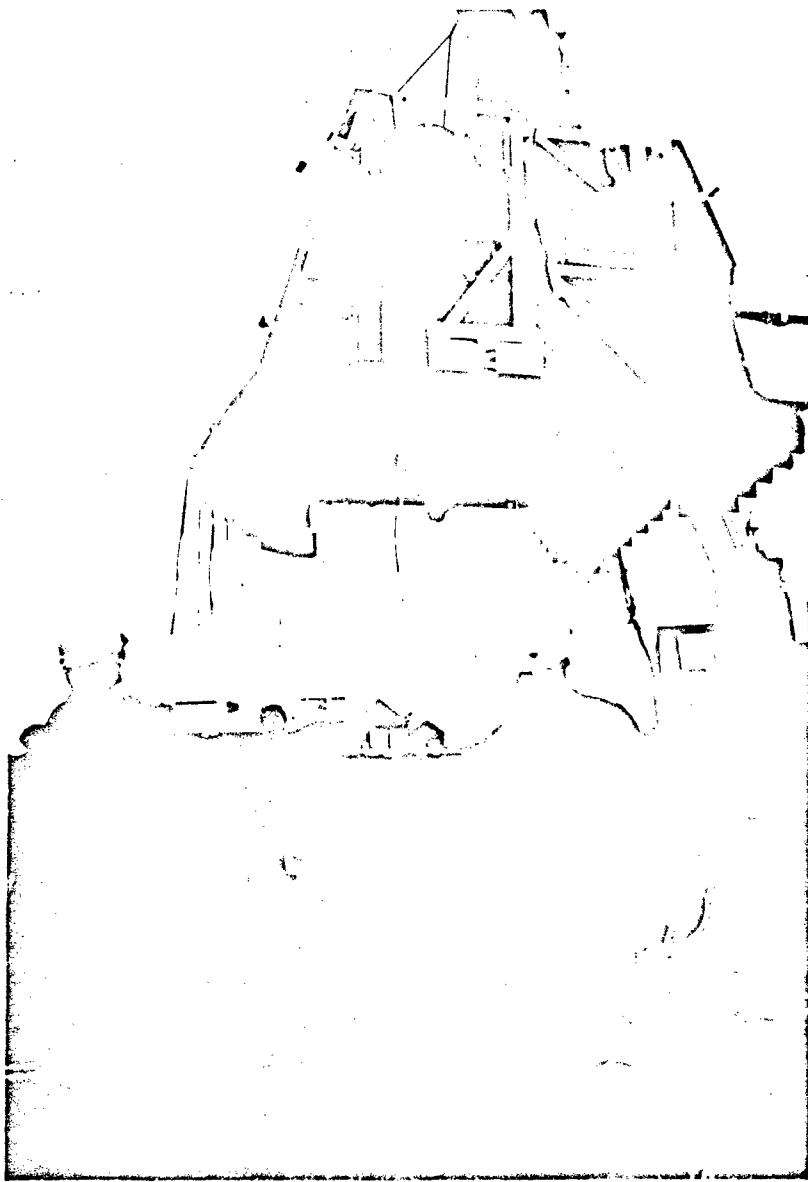


Figure 1. ABLE Payload on Day of Launch

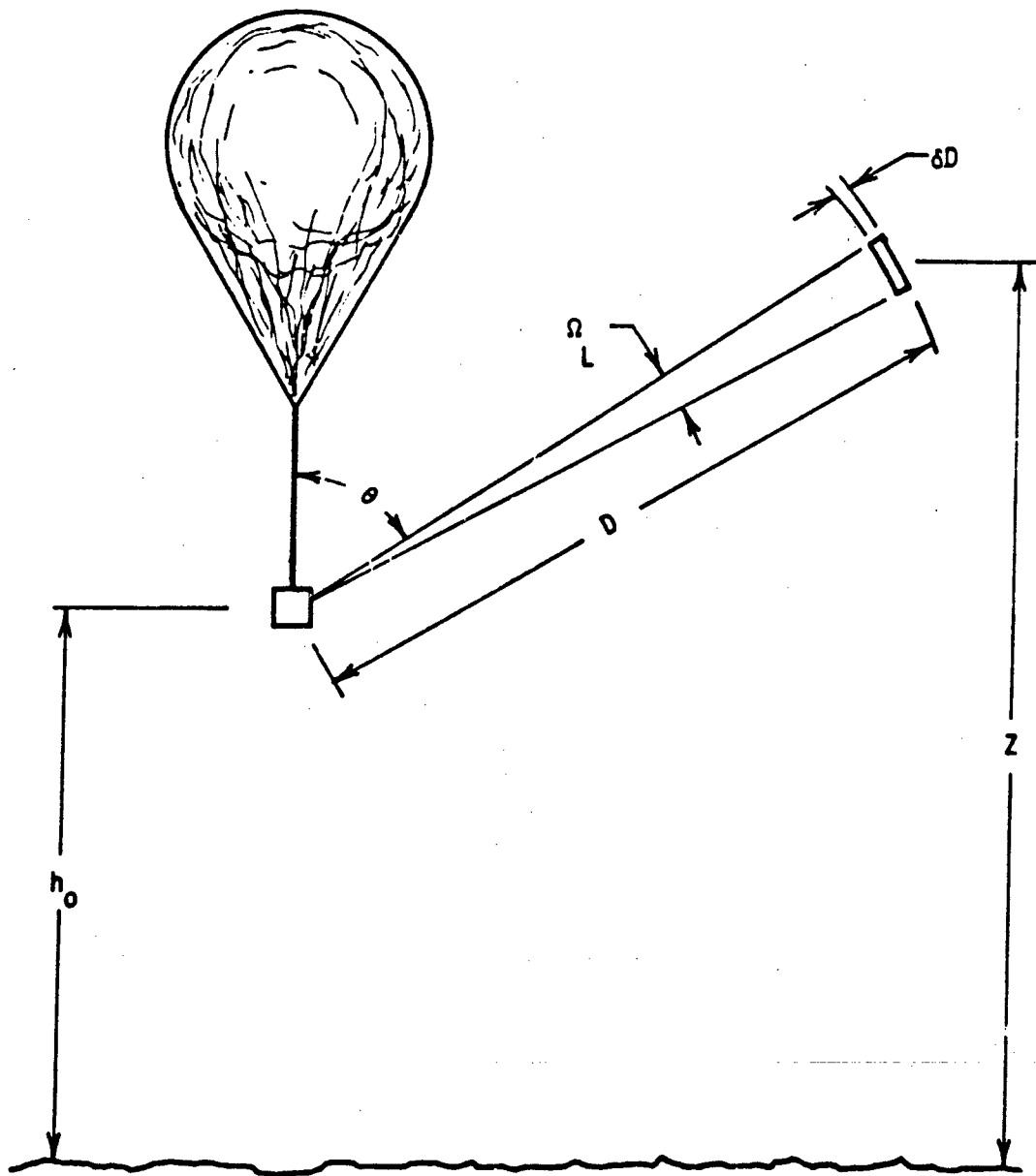


Figure 2. Predicted Signal Level Calculation Geometry

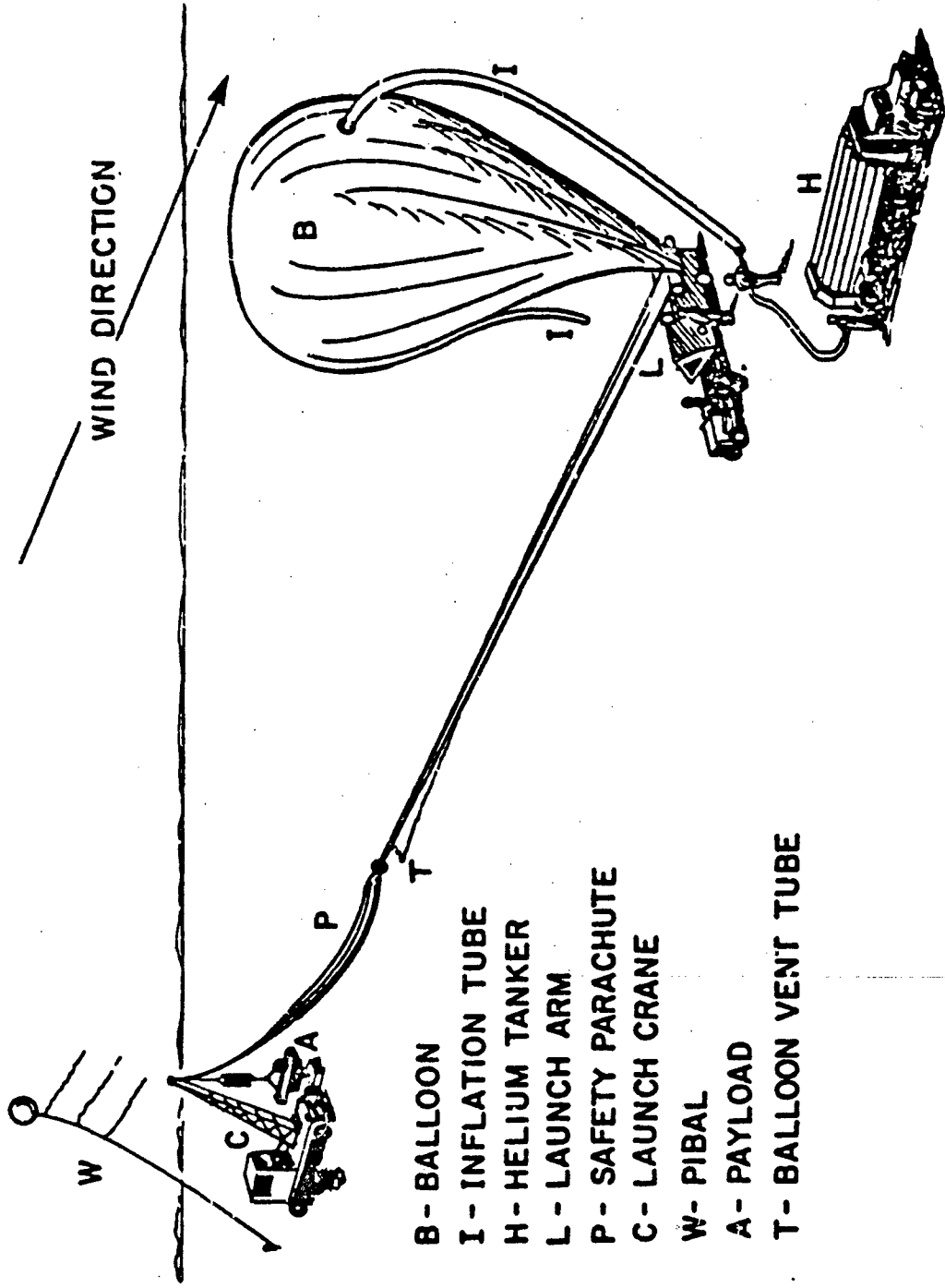
where e_λ is the energy in the laser pulse at wavelength λ , $h\nu$ is the photon energy, f is the fraction of the atmospheric element dV visible to the detection system, σ_λ is the Rayleigh scattering cross section at 180° , $N(z)$ is the atmospheric molecular number density vs altitude, A is the area of the collecting mirror, and T_λ is the atmospheric transmission for a photon traversing a path length of $2D$ at the specified altitude and zenith angle.

To separate the Rayleigh backscatter from the aerosol Mie backscatter, a two wavelength lidar is required. In reference 2, the two proposed wavelengths were the fundamental (1064 nm) and the frequency-tripled (355 nm) outputs of a Nd:YAG laser. However, the manufacture of the proposed detector for the 1064 nm was discontinued. For this reason, the effect on the density data of using other detectors and/or the frequency-doubled (532 nm) output of the Nd:YAG laser was investigated. The statistical errors in the Rayleigh backscatter measurement data for two measurement techniques, 1064 nm/355 nm and 532 nm/355 nm, were calculated and compared. It was shown that by using the 532 nm/355 nm technique with an S-11 532 nm detector, the resulting density data would have significantly less statistical error than that which would be obtained by using the 1064 nm/355 nm technique with a cooled S-1 detector at 1064 nm.

To examine the performance of the two detectors being considered for aerosol correction, S-11 at 532 nm and S-1 at 1064 nm, the lidar backscatter prediction code was run. The counting statistics thus obtained using the S-1 photomultiplier response at 1064 nm do not warrant using it for the aerosol correction. In addition, the added complexity of cryogenic cooling required for this detector would be eliminated, and therefore, an uncooled S-11 photomultiplier at 532 nm was used as an aerosol correction detector.

The requirement for low background levels in the two spectral bands of interest dictated that the data flight be at night. Thus the balloon launch (Figure 3) was scheduled for around sunset. The selection of a launch time also depends upon the low level ground wind conditions, wind shear, and high altitude winds. It is desirable to keep the payload flight path over the controlled airspace of White Sands Missile Range (WSMR) for as much of the flight as possible. Thus, low velocity winds are a launch criterion. As long as the payload is over the controlled airspace, the lidar can be directed downward, thereby providing the most complete density distribution data.

Briefly the plan of the flight phase of the ABLE experiment was as follows: The balloon will be launched with the lidar in standby mode. At an altitude of



- B - BALLOON
- I - INFLATION TUBE
- H - HELIUM TANKER
- L - LAUNCH ARM
- P - SAFETY PARACHUTE
- C - LAUNCH CRANE
- W - PIBAL
- A - PAYLOAD
- T - BALLOON VENT TUBE

Figure 3. Balloon Launch Preparation

paration for firing. All firing of the laser is to be commanded by the AFGL technical contract monitor, Dr. D. E. Bedo. To help control the coolant temperatures, the laser can be fired into a dump when the pointing mirror is in the horizontal mode. When the payload reaches an altitude of 30 kft, the pointing mirror will be commanded to direct the lidar to the upward mode, laser firing will begin and backscatter data taken. When the balloon flight is over the restricted area of WSMR, the pointing mirror will be commanded to the downward mode, and backscatter data taken until the balloon drifts out of the restricted area. At that time, data taking will be confined to the upward mode only.

After a mission operating time of approximately six hours at float altitude, the lidar system will be turned off and the pointing system slewed into stow configuration. The balloon will be valved down to lower altitude (about 23 km) and the balloon ruptured on command. The payload parachute will open and the payload will drift down and impact on the ground. An on-board beacon transmitter will lead search aircraft to the downed payload, and experiment project personnel will be guided to inspect the payload to determine that it is in a nonhazardous condition. The payload will then be transported back to the payload build-up area.

During the time of flight, other experiment personnel will be in the balloon mission control center evaluating data quality and instrument performance from the real-time readout of the raw telemetry data. In addition, lidar experiment data will be displayed in real time to provide experiment personnel with sufficient data to permit a preliminary evaluation of the mission's scientific success.

3. SYSTEM DESIGN

The ABLE experiment payload consists of a dual frequency lidar system for measuring atmospheric backscatter signals at 355 and 532 nm as a function of altitude from ground level to 70 km. The basic lidar specifications are listed in Table 1. The principal components of the payload are as follows:

1. A payload structure.
2. A Nd:YAG laser transmitter.
3. A telescoped receiver with 355 and 532 nm detectors.
4. A command-controlled optical pointing system.
5. A payload thermal control system.
6. Telemetry, command, and power systems to support the experiment.

These components are discussed individually in the sections that follow.

TABLE 1
BALLOONBORNE LIDAR SPECIFICATIONS

PAYLOAD			
WEIGHT	2112 LB. (WITHOUT BALLAST)		
SIZE	2.8 X 2.8 X 1.5 METERS		
POWER	1800 W (WITHOUT T/M)		
LIDAR			
TRANSMITTER			
WAVELENGTHS	355	532	NM
ENERGY/PULSE (TYPICAL)	0.03	0.15	J
DIVERGENCE	2.5	2.5	MR
REPETITION RATE	10PPS		
PULSE WIDTH	16 NSEC		
RECEIVER			
COLLECTING OPTICS	DALL-KIRKHAM CASSEGRAIN		
COLLECTING AREA	1875 CM ²		
FIELD OF VIEW	4 MILLIRADIANS		
DETECTORS	PMT'S AT AMBIENT T		
DESIGN POINTING ACCURACY	0.2 MR		

3.1 Payload Structure

The ABLE payload structure is shown in Figures 4 and 5, which are forward and aft views taken during final assembly. The trussed structure is of welded aluminum angle beam, and has a central deck used principally as an optical bench, the main purpose of the structural frame being to provide a rigid, stable platform for the lidar optics. Other important components of the payload structure are the pressure chambers which house the laser, the laser power supply, computer, and the receiver detectors, and maintain them at one atmosphere absolute pressure during flight.

The payload structure has a low center of gravity and a wide support base in order to withstand substantial lateral forces without toppling either during a parachute landing or whenever a recovery helicopter lowers it to the ground. To achieve the required stability, the central part of the structure is a welded aluminum frame with four sides and three decks. The middle deck is dedicated to mounting the optical instruments. It is a rigid optical bench that allows positioning and alignment of the lidar transmitter and receiver system. On each of the four sides of the structure, there are four diagonal members fastened to welded gussets in such a way that they contribute substantially to the torsional stiffness of the frame.

Surrounding the central frame is a series of roll bars bolted to the sides of the frame, thus providing protection to the lidar in case of crash landing by dissipating the descent kinetic energy into work to deform the roll bar members. In addition, they provide space for the batteries, ancillary equipment, and telemetry instrumentation. They also provide support for crush pads, which are energy-absorbing devices that utilize the ability of crushing to absorb the force of impact. Prior to frame fabrication, a quarter scale model of the payload, shown in Figure 6, was assembled to check the design. Next, a structural analysis (Appendix A) of the payload was performed using a computer code ADINA for a three-dimensional frame divided into nodes and connecting elements. All loads were considered to be applied to the nodes. Acceleration forces which were considered included the following:

1. 2 g's at launch (stress level to be within Hooke's Law).
2. 10 g's at parachute deployment (payload survival).
3. 10 g's on landing (some damage to roll bars).

In addition, a thermal analysis was performed to study the effect on the lidar

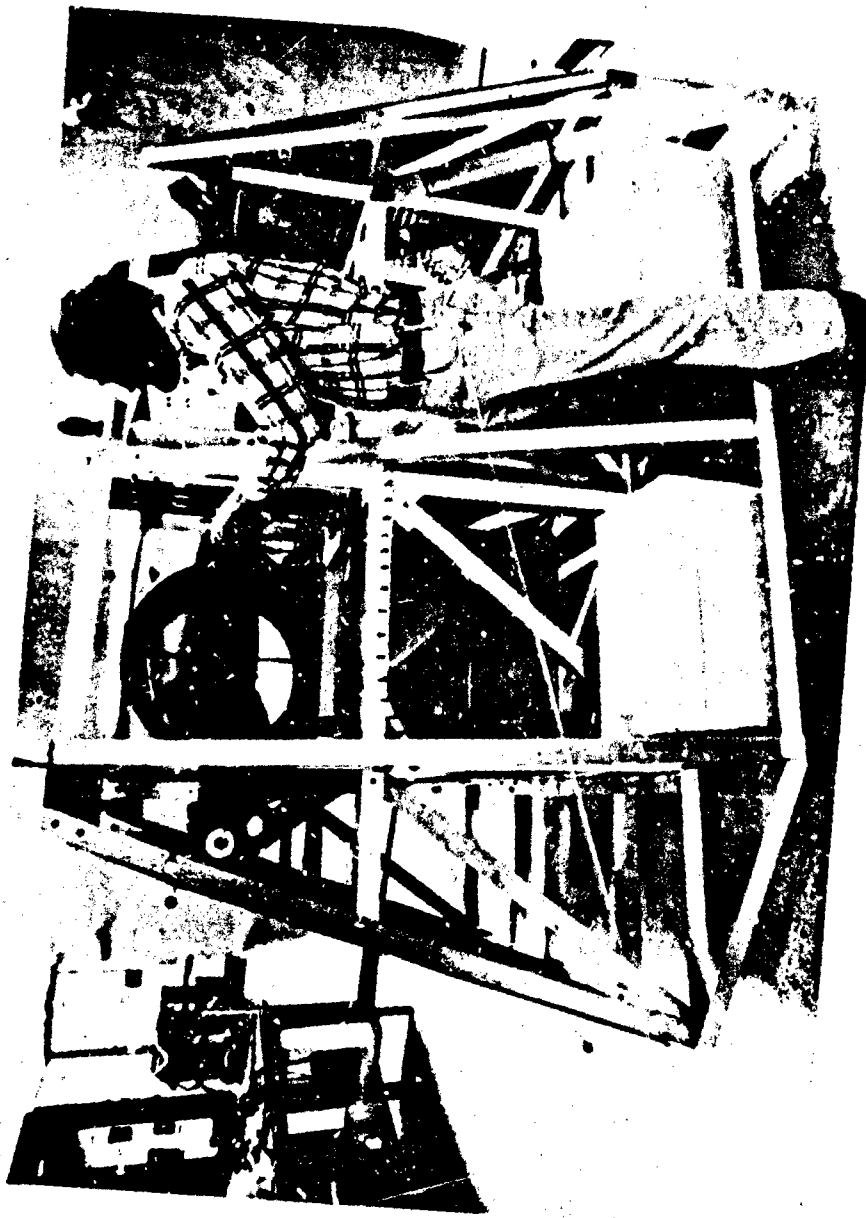


Figure 4. ABLE Payload during Final Assembly. Forward View

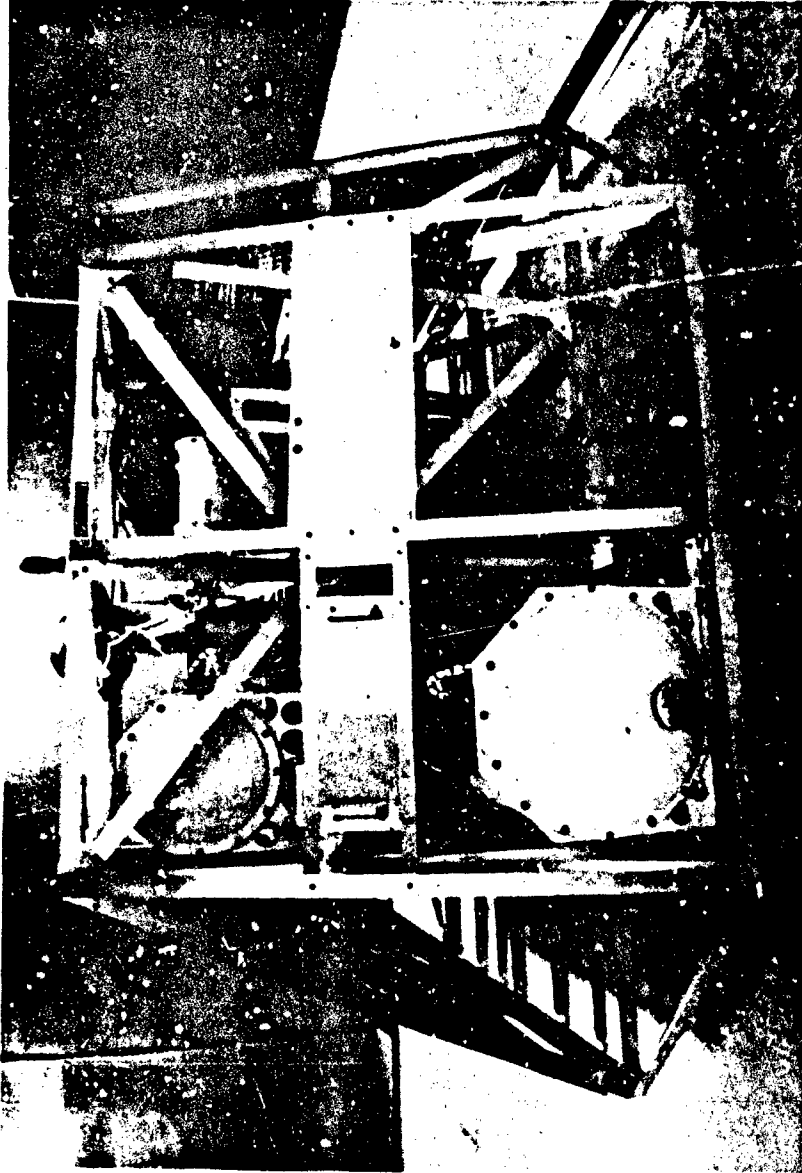


Figure 5. ABLE Payload during Final Assembly, Aft View

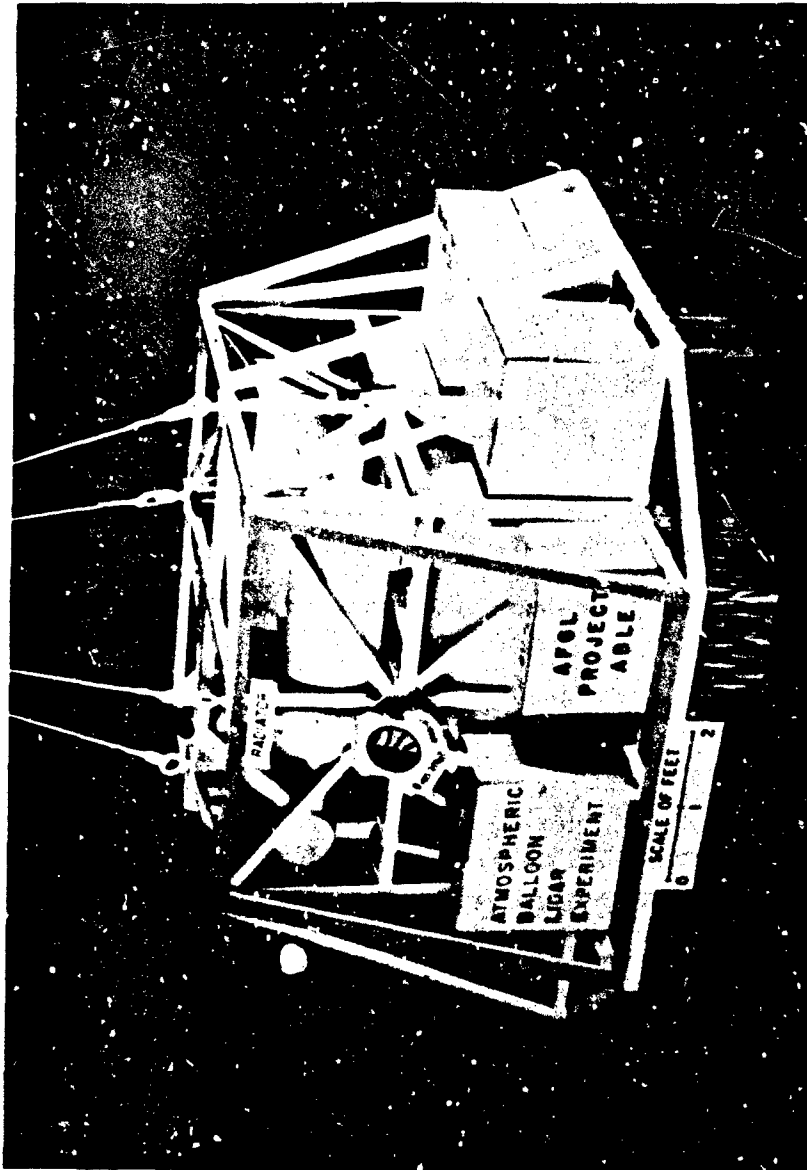


Figure 6. ABL Payload, Quarter-scale Model

optical alignment of a thermal gradient across the frame.

3.2 Transmitter

The transmitter consists primarily of an International Laser Systems (ILS) Nd:YAG laser. The laser was government furnished equipment, and its test and acceptance procedures by government personnel were supported by Visidyne personnel in accord with the contract work statement. The results of these tests are summarized in Appendix B. A laser energy monitor designed and manufactured by Visidyne was mounted on the laser optical bench to measure the laser output at all three wavelengths during the experiment.

3.2.1 Laser

The balloonborne lidar experiment required a Nd:YAG laser which is frequency doubled and tripled to provide coaxial outputs at 1064 nm, 532 nm, and 355 nm. The characteristics required of this laser are as follows:

1. The system must be capable of being powered by 28 Vdc.
2. The system must be of a lightweight, rugged design with a compact configuration capable of being packaged for balloonborne operation.
3. The unit should be capable of being modified, as required, for this specific application.

A laser system meeting these criteria, and used to develop this design, was a variation of the ILS-104. The laser is shown in Figure 7, and an optical layout of the laser is shown in Figure 8. The detailed specifications are given in Table 2.

The laser uses an oscillator and two amplifiers to obtain the specified power levels. The oscillator (and amplifier) rods are pumped by xenon flashlamps. After a preset delay, typically 130 μ sec, the Pockels cell Q-switch is triggered. A 15 nsec wide pulse of 1064 nm radiation is dumped from the oscillator through amplifiers 1 and 2 resulting in a 700 mJ pulse of 1064 nm radiation.

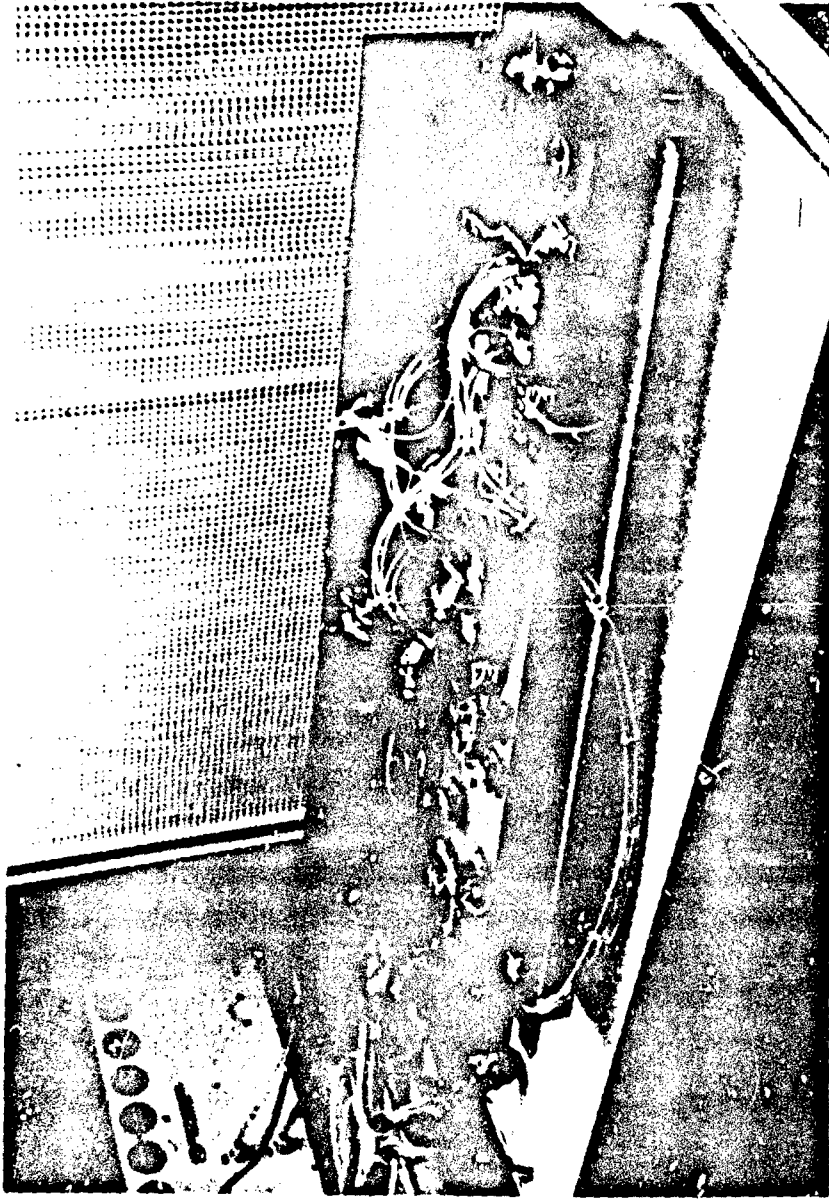


Figure 7. Nd:YAG Laser prior to Payload Assembly

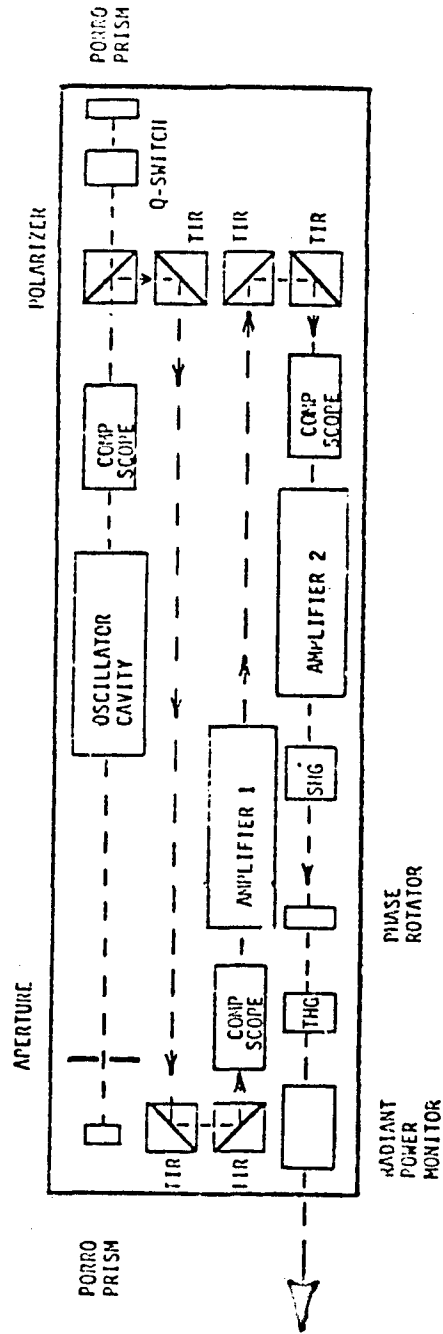


Figure 8. Laser Optical Layout

Table 2. PROJECT ABLE LASER SPECIFICATIONS

Laser Model:	ILS 104-10 with DC Power Supply		
Type:	Nd:YAG		
Output Wavelengths:	1064 nm	532 nm	355 nm
Typical Simultaneous Output Energies:	190 mJ	153 mJ	37 mJ
Exit Beam Divergence:	<u><2</u> mr	<u><1</u> mr	<u><1</u> mr
Polarization:	Horiz.	Vert.	Horiz.
Amplitude Stability: (Pulse to Pulse)	<u><3%</u>	<u><5%</u>	<u><10%</u>
Repetition Rate:	10 pps		
Pulse Width:	15 nsec		
Pulse Jitter (Sync to Pulse)	<50 nsec		
Exit Beam Diameter:	6.35 mm (Beams are coaxial)		
Coolant:	30% Deionized Water - 70% Glycol		
Coolant Flow:	0.5 gal/min typ. ±0.25 gal/min		
Coolant Pressure:	12 psig max.		
Maximum Coolant Temperature at Outlet	55°C		
Minimum Coolant Temperature at Inlet	5°C		
SHG Crystal:	CD*A		
THG Crystal:	RDP		

The 1064 nm output from the flashlamp-pumped, Q-switched Nd:YAG laser enters a second harmonic generation (SHG) crystal which outputs orthogonally-polarized 1064 nm and 532 nm radiation. A quartz rotator plate brings these two wavelengths back into the same plane before they enter a third harmonic generation (THG) crystal. The THG crystal mixes the 1064 nm and its second harmonic to produce 355 nm third harmonic radiation. All three wavelengths are present in the coaxial output beam.

In order to achieve maximum efficiency of the tripler, the SHG and THG crystals must be tuned (i.e. peaked) in both angle and temperature. For the balloonborne lidar system, the SHG and THG crystals are maintained at constant temperature by ovens. Two-axis angle tuning of these crystals is done by using motordriven micrometers. These are operated through the uplink command system.

3.2.2 Laser Energy Monitor

The function of the laser energy monitor (LEM) is to monitor laser beam energies continuously during operation. Figure 9 details the device components. The incoming laser beam passes through the device and is incident on the beam splitter. The beam splitter is antireflection coated so that only one or two percent is removed from the laser beam.

The LEM has several advantages over existing laser energy monitors as follows:

1. **Calibration Stability.** Usually, laser energy monitors rely on scattering from imperfections in a glass or silica window mounted in the laser beam. The fraction of scattered radiation is extremely small, on the order of 10^{-4} or 10^{-5} . The calibration of such a monitor can be affected drastically by an additional surface scratch or a piece of dust. The LEM samples a much larger fraction so that additional surface defects do not appreciably change the calibration.
2. **Uniformity of Sampling.** Typical energy monitors which rely on scattering from small imperfections do not sample the laser beam cross section uniformly. Therefore, if the beam cross section pattern should change or shift, the monitor would give an erroneous reading, and in fact, might have been giving erroneous readings all along. The LEM uniformly samples the entire beam cross section at all times so that it is completely unaffected by any variations in the beam pattern.
3. **Minimal Effects on Laser Operation.** Energy monitors which have reflecting surfaces normal to the laser beam will reflect some of the signal back into the laser itself. This can have a drastic effect on the operation of the laser. Monitors which measure signals scattered normal to the laser beam may give incorrect readings because of beam polarization, or they may reflect an

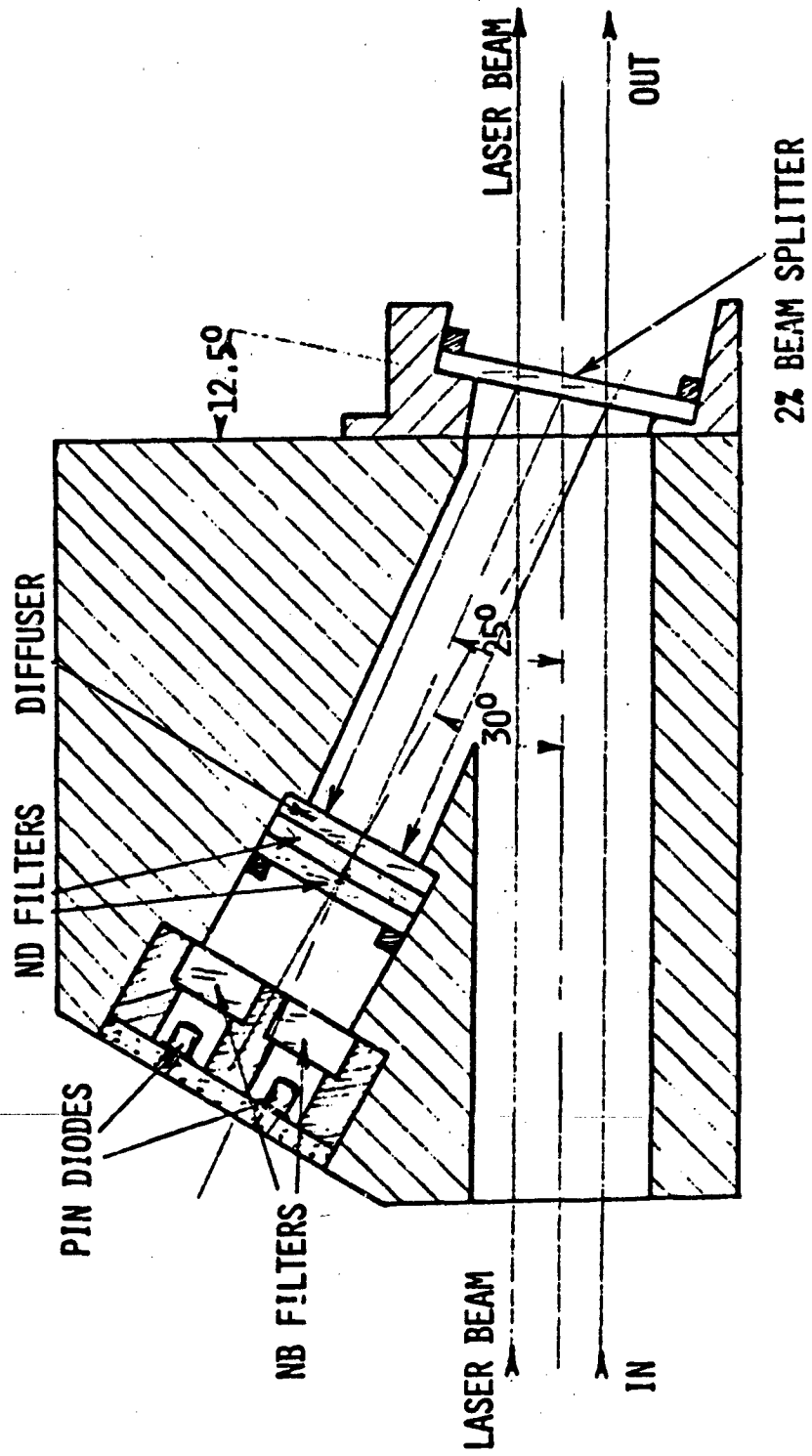


Figure 9. Laser Energy Monitor (LEM) Details

anomalously large fraction of the beam energy if the beam polarization is parallel to the reflecting surface. The LEM practically eliminates all these disadvantages by mounting the beam splitter at a small angle (12.5°) of incidence to the laser beam. Therefore, no energy is reflected back into the laser, and the beam polarization does not affect the measurements and is not itself appreciably altered.

3.2.3 Transmitter System

The laser firing is controlled in flight by a set of independent functions, as follows:

1. Laser firing is enabled only when an uplink laser fire command is being received.
2. A baroswitch disables laser firing below a preset altitude. The altitude setting is determined by range/eye safety parameters.
3. A clock timer automatically disables laser firing after a preset time-from-launch has elapsed.
4. An uplink command will arm/safe the laser high voltage power supply.
5. Interlocks are provided to prevent laser firing when the pointing mirror is not properly positioned.

The laser and its power supply are enclosed in two interconnected chambers that maintain the system at a pressure of 1 atm throughout the flight. Figure 10 shows the laser mounted in its pressure chamber.

3.3 Receiver

The lidar receiver consist principally of the following assemblies:

- a. Dall-Kirkham Cassegrain telescope assembly
- b. beam splitter and filter assembly
- c. 355 nm detector assembly
- d. 532 nm detector assembly

The receiver optics, shown in Figure 11, includes a large aperture collector, beam splitters to separate the 355, 532, and 1064 nm wavelengths, and a pair of narrowband interference filters to eliminate the out-of-band background radiation. The lidar receiver optical specifications are summarized in Table 3.

3.3.1 Telescope Assembly

The receiver collector is a Dall-Kirkham^[3] Cassegrain telescope as-

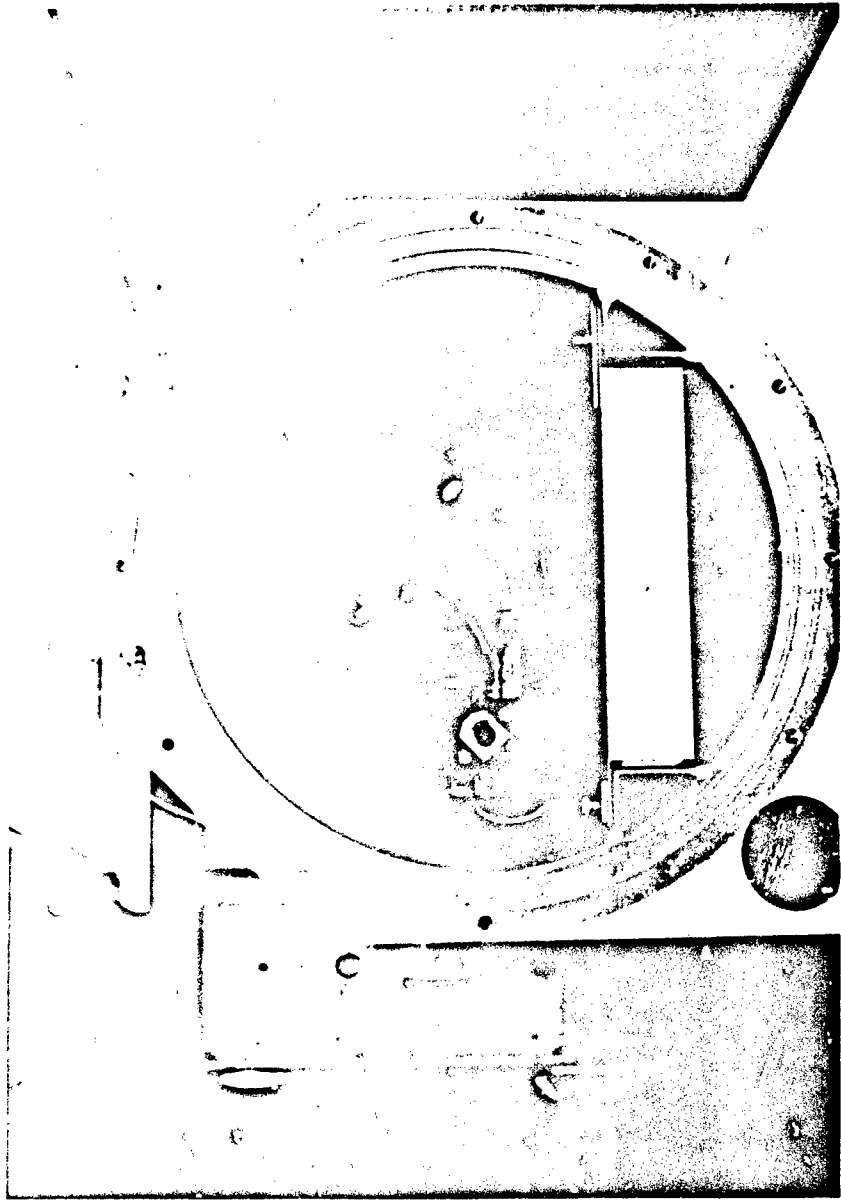


Figure 10. Laser Mounted in Payload Pressure Chamber

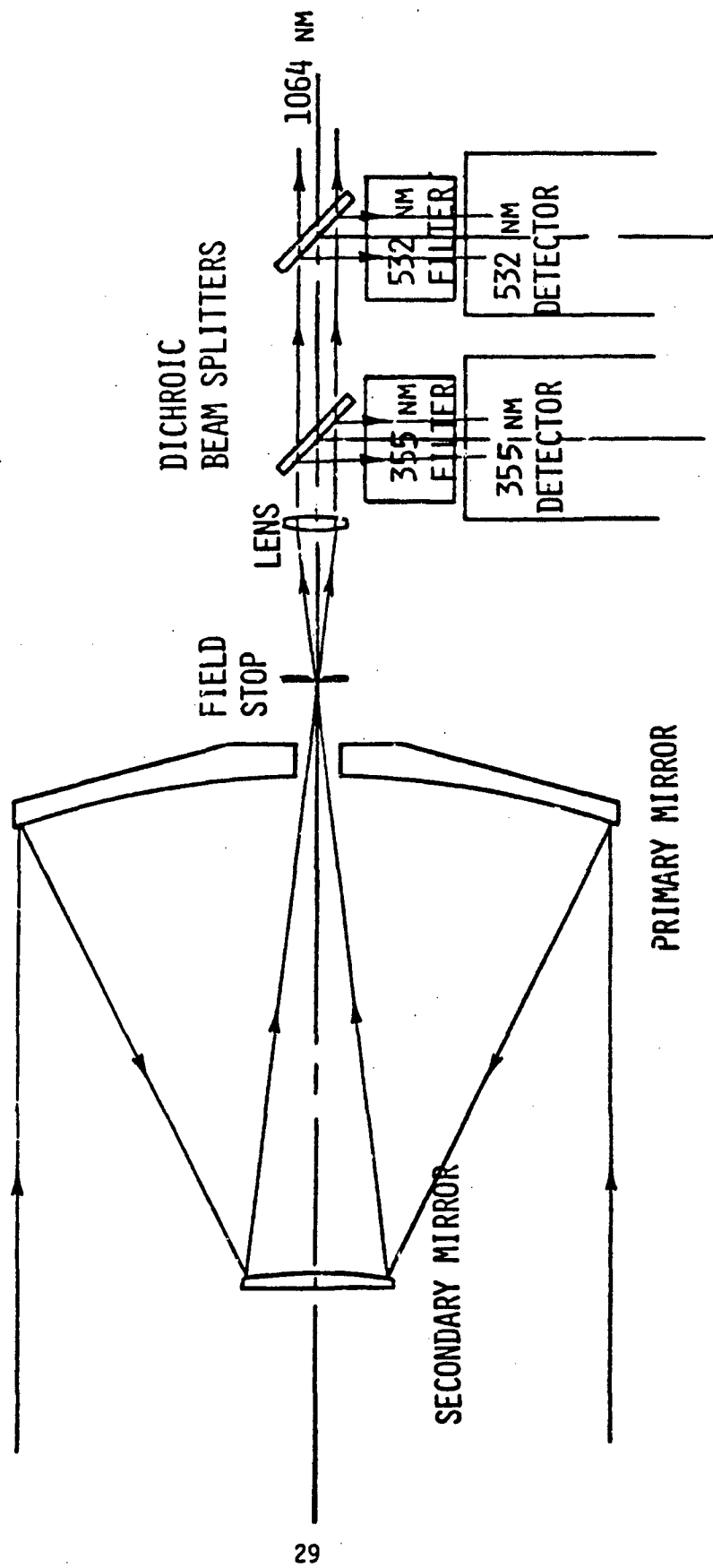


Figure 11. Receiver Optics Layout

Table 3. LIDAR RECEIVER OPTICAL SPECIFICATIONS

<u>Field of View</u>	4 m _r
<u>Telescope</u>	
Type	Cassegrain, Dall-Kirkham
f/no.	5.0
Primary Mirror	
Material	Aluminum
Diameter	50.4 cm
Coating	Aluminum + SiO
Secondary Mirror	
Material	Aluminum
Diameter	10.1 cm
Coating	Aluminum + SiO
Effective Collecting Area	1875 cm ²
Effective Focal Length	241.3 cm
Reflection	
at 355 nm	0.79
at 532 nm	0.74
<u>Relay Lens</u>	
Material	Fused Silica, UV Grade
Type	Plano-convex
Focal Length	6.99 cm
Diameter	3.81 cm
f/no.	1.8
<u>Beam Splitters</u>	
Material	BK-7 Glass
First Beam splitter	
355 nm Reflection	95 percent
532 nm Transmission	95 percent
Second Beam Splitter	
532 nm Reflection	95 percent
<u>Interference Filters</u>	
Clear Aperture	4.5 cm
Bandpass	
355 nm	22 Å
532 nm	10 Å
Transmission	
355 nm	0.16
532 nm	0.54

sembly having an essentially ellipsoidal primary mirror and a spherical secondary. This type of Cassegrain telescope is easier to manufacture and simpler to align than a true Cassegrain. The disadvantage of the Dall-Kirkham system is that the off-axis coma is several times greater than that of the true Cassegrain.^[4] However, one of Visidyne's ray tracing programs, RAYTRAC, verified that a true Cassegrain system is about fifty times better in coma than that required by the proposed lidar system, so that a Dall-Kirkham system was more than adequate for the Project ABLE application. The optical data of the ABLE telescope assembly are listed in Table 4.

The receiver telescope optics were mounted in the telescope baffle assembly by the mirror fabricator, Optical Systems Technology Incorporated (O.S.T.I.). They were aligned and focused at that time by O.S.T.I. personnel with the procedures observed by Visidyne personnel.

**Table 4. DALL-KIRKHAM OPTICAL SYSTEM DATA
(Linear dimensions in inches)**

CA	= Clear Aperture	= 19.75
f_p	= Primary focal length	= 20.00
$f_p/\text{No.}$	= Primary f/Number = f_p/A	= f/1.0
d	= Vertex separation	= 16.0
p	= ($f_p - d$)	= 4.
p'	= Back focal length	= 19.0
M	= Magnification = p'/p	= 4.75
E.F.L.	= Effective Focal Length = $f_p(m)$	= 95.0
B.F.D.	= Back Focal Distance	= 3.0
F/No.	= System effective F/No. = EFL/A	= f/4.8
b	= Primary vertex to F'	= 3.0
Rp	= Primary vertex radius = $f_p(2)$	= 40.0
Rs	= Secondary vertex radius = $2pp'/(p'-p)$	= 10.118
Dp	= Primary Mirror Diameter	= 20.0
Ds	= Secondary Mirror Diameter	= 4.5
Ds/Dp	= Obscuration Ratio	= 0.25
B.C.D.	= Blur Circle Diameter	= 0.018
P_{ID}	= Primary Perforation Diameter	= 3.0
Zp	= Primary Sagitta	= 1.229
Zs	= Secondary Sagitta	= 0.253

The telescope assembly, including the field stop, is on a vertically adjustable mount. A flexible, light-tight coupling connects the telescope and beam-splitter-filter assemblies. When this coupling is removed, the receiver field-of-view can be observed during focusing and pointing adjustments.

3.3.2 Beam Splitter and Filter Assembly

The beam splitter and filter assembly contains a relay lens which focuses the field stop into the detector assemblies, two dichroic beamsplitters, and two temperature-controlled narrowband filters. Specifications for these optical components were given in Table 3.

The dichroic beam splitters effectively separate the 355 and 532 nm signals into the respective detectors while the 1064 nm signal is transmitted by both beam splitters. The two narrowband interference filters, one peaked at 355 nm and one at 532 nm, are mounted in front of the appropriate PMT detectors in the receiver. The chosen bandwidths of these filters are a compromise between a width narrow enough to reject out-of-band background radiation and one wide enough to have reasonable peak transmissions at the wavelengths of the backscattered signals. The interference filters in the receiver have passband drift coefficients of 0.007% per °C, and therefore they are mounted in temperature-controlled ovens. The transmission curves of the filters (supplied by DayStar Filter Corp.) were verified at the design temperature by an independent source and witnessed by Visidyne personnel.

3.3.3 Detector Assemblies

The ABLE lidar receiver detectors are photomultipliers. The two photomultipliers, together with their high voltage power supplies and electronics, are packaged in individual hermetically-sealed housings. EMI photomultiplier detectors were selected because gating performance data and circuitry and maximum rated cathode photocurrent data are available for this photomultiplier. The detector specifications are listed in Table 5.

A simplified schematic diagram of the detector electronics is shown in Figure 12. The photomultipliers were operated in the current measurement mode to provide the maximum dynamic range. Three gain channels, each differing by a factor of 20, were used. The signal from each channel was digitized to 10 bits at 1 MHz sample rate. Thus an effective dynamic range of 4×10^5 was obtained with a minimum signal-to-quantization noise ratio of 50.

TABLE 5. DETECTOR SPECIFICATIONS

Type	Photomultiplier EMI 9815A	
Photocathode	Bialkali	
Gain	3.1×10^5	
Range Gating Method	Dynode 1 Switch	
Amplifier Dynamic Range	<u>Equivalent counts</u>	
	<u>Min</u>	<u>Max</u>
Hi Gain	0.5	256
Med Gain	10	5120
Low Gain	200	1.30×10^5
Dark Count Rate	150 Counts/Sec	
Probability of a Dark Count in a Range Bin	1.5×10^{-4}	
Range Bin Length	150 meters	

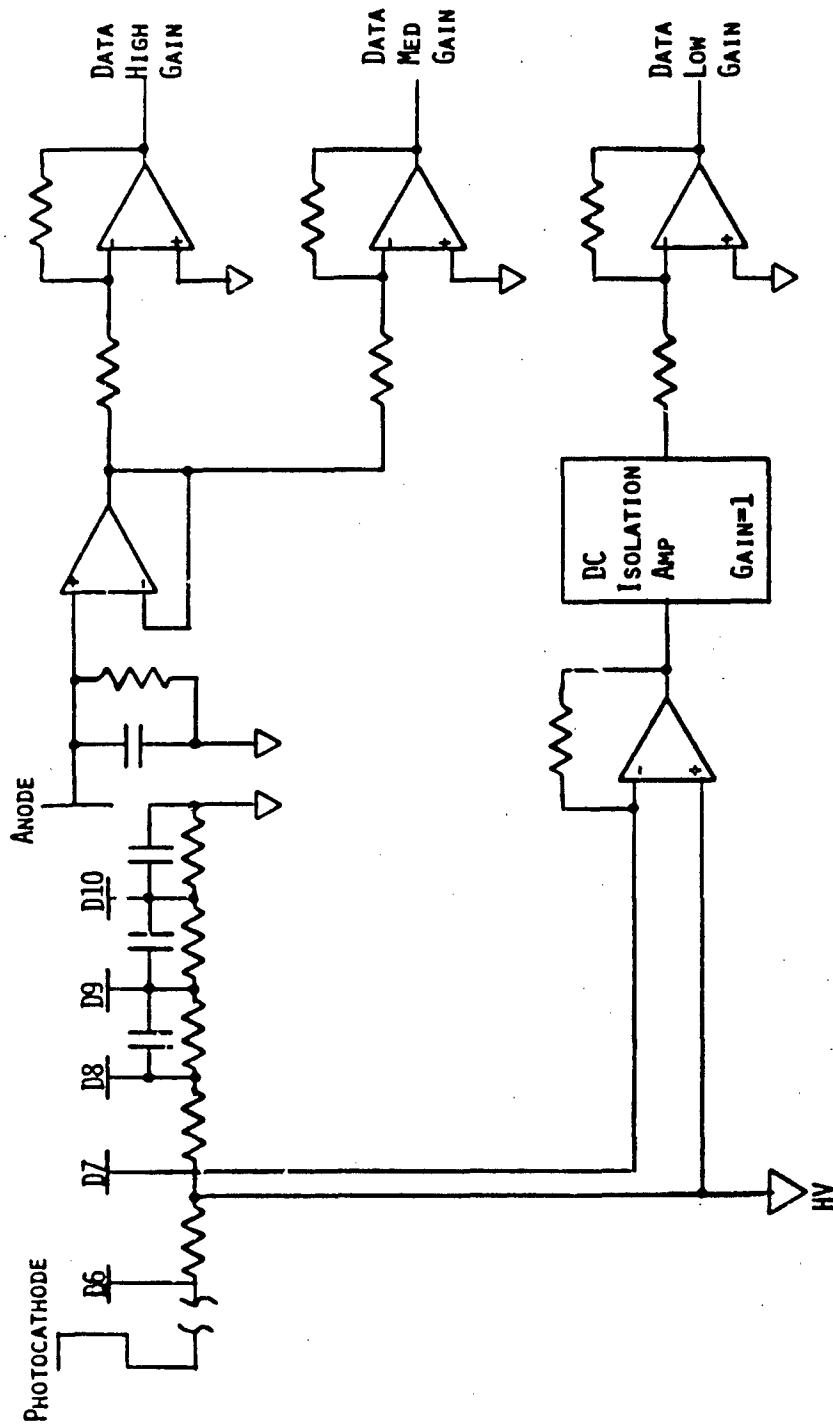


Figure 12. Detector Electronics, Simplified Schematic

3.4 Optical Pointing System

The pointing mirror system, shown in Figure 13, is composed of a laser mirror and a receiver mirror connected rigidly to a commandable, motor-driven shaft. The shaft is supported at only two points, one at the gearbox bearing and the other at a self-aligning ball bearing adjacent to the receiver mirror. Beyond this bearing, the shaft supports the laser mirror on a cantilever beam. The cantilever has been designed to minimize the deflections of the pointing mirrors. This is accomplished by using the weight of the receiver mirror to counterbalance the deflection of the cantilever beam.

The drive mechanism rotates the receiver pointing mirror and the laser pointing mirror to the desired position. It includes a stepping motor, a planetary gear train, a tee drive, an optical encoder that monitors the position of the mirrors, and mechanical limit switches. The drive is controlled through the CAMAC electronics. An optical encoder is hard mounted to the free side of the tee drive allowing a continuous monitoring of the position of the pointing system.

Since the pointing mirror system is supported at only two points and most of the shaft is cantilevered, the mirrors translate parallel to themselves under the effect of a thermal variation without changing the alignment. The aluminum shaft is 3" in diameter with a 0.125" wall, and is stiff enough to maintain the desired alignment.

The laser pointing mirror has a multilayer dielectric coating which is able to reflect the laser beam without being damaged, while the pointing mirror has the same coating as the receiver telescope.

3.5 Thermal Control System

The function of the thermal control system is to maintain the ABLE subsystem temperature within the defined operational limits during a balloon flight. The laser and its power supplies generate approximately 1000 watts of heat during operation. This heat must be eliminated from the payload system. The most efficient method to remove the waste heat is by radiation to space. The design of the thermal control system is complicated slightly by the laser requirement of using a deionized cooling fluid.

The selected laser for the lidar payload comes equipped with a cooling system which must be integrated by means of a heat exchanger into a secondary cooling system. This secondary system then carries the unwanted heat from the laser cooling system to the radiator which dissipates the heat to space. The

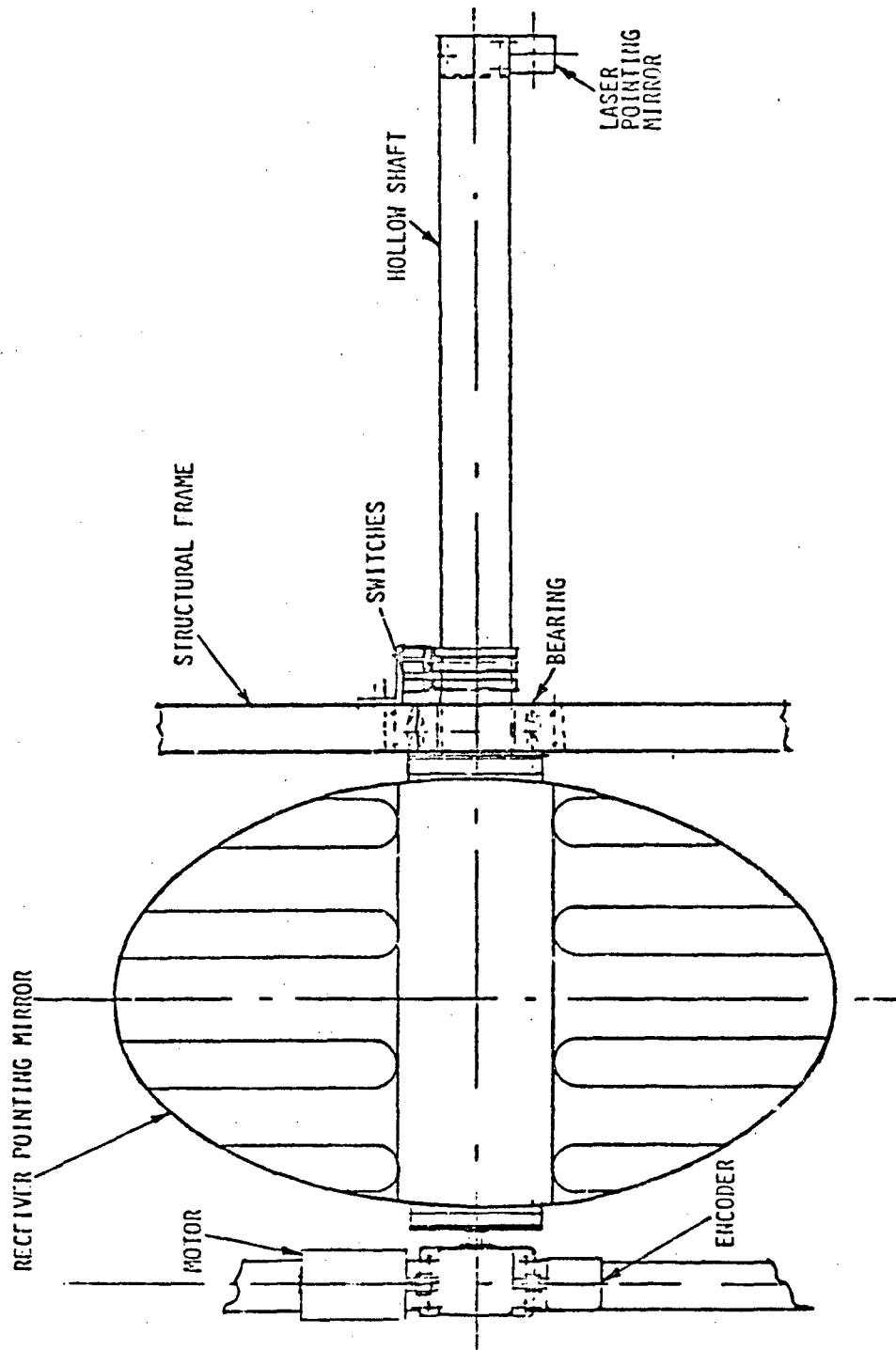


Figure 13. Pointing Mirror System

laser system should be maintained within a maximum allowable temperature of 35°C and a minimum allowable temperature of 5°C.

The cooling system schematic is indicated in Figure 14 and its components listed in Table 6. The primary loop is the laser cooling system which contains deionized water/glycol and is sealed and maintained separate from the secondary cooling loop. The secondary loop radiates the excess heat to outer space by using a water/glycol mixture flowing through two large stainless steel radiators. A fin-and-tube aluminum heat exchanger with fans is also utilized.

Figure 14 indicates the temperature in degrees Fahrenheit expected at various points. These temperatures are based on calculations done by Visidyne and by Lytron Inc. Quick disconnects are used where applicable. A special low temperature ethylene vinyl acetate tubing is used for the plumbing between the laser and the heat exchanger.

At the payload operational altitude of 100,000 feet, a simple flat plate type design radiator radiating to space was determined as the best method of dissipating heat. This was based on data taken by Visidyne on similar balloon flight operations with the Project BAMB payload. When the average temperature of the radiator is 37°F (3°C), it will reject heat at about 26 watts/ft². Since 1000 watts must be dissipated, the radiation area required is then 38 ft². The radiator temperature used here is based upon experimental measurements of a heat exchanger panel on the BAMB payload at float altitude. The ABLE payload has two radiators of approximately 25 ft² each mounted on opposite sides of the payload. They are each made of two stainless steel sheets 0.04" thick welded at the edges and expanded into a quilted pattern to create a coolant flow path between the plates. The outer sides of the radiators are painted gloss white having an absorptivity of 0.2 for solar radiation and an emissivity of 0.85 at the radiator temperature.

Three temperature switches are used to control the cooling system. One switch is set at 35°C to turn off the laser to avoid overheating. When the temperature drops (no heat input from the inactive laser), the laser can be turned on again from the ground control. A second switch is set at 10°C to turn off the laser cooling system pump if the cooling fluid drops below this temperature. The third temperature switch is also set at 10°C in the power supply cooling air flow. When this air flow temperature drops below 10°C, the two muffin fans will be shut off and the heat generated by the two power supplies allowed to raise the air temperature to the point where the cooling fans are

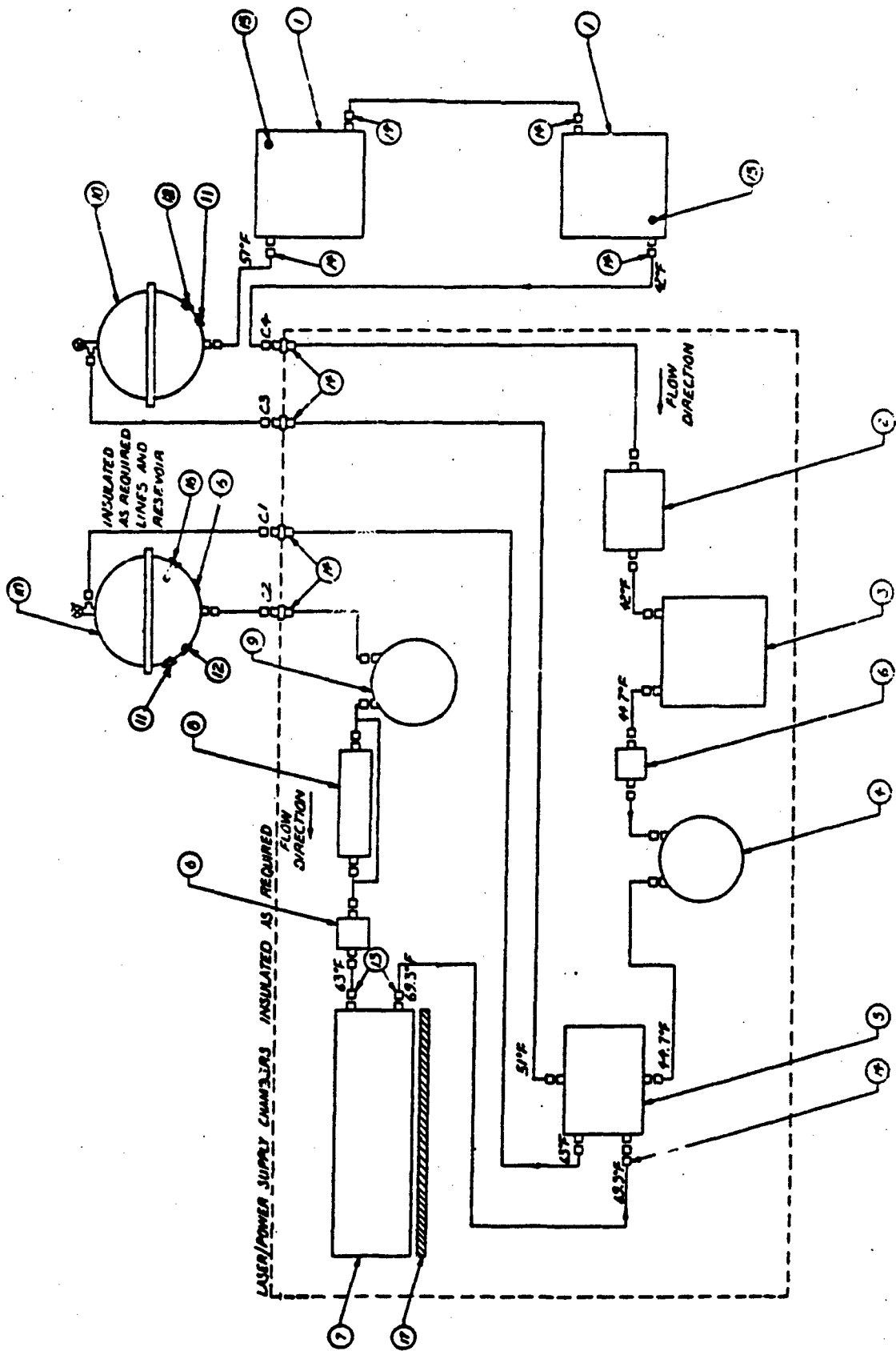


Figure 14. Lidar Cooling System

Table 6. LIDAR COOLING SYSTEM COMPONENTS

<u>ITEM NO.</u>	<u>QTY. REQ'D</u>	<u>DESCRIPTION</u>
1	2	RADIATOR
2	1	FLOW SWITCH, MODEL 150
3	1	LIQUID - AIR HEAT EXCHANGER
4	1	GEAR PUMP, MODEL 118-641-00K
5	1	PASSIVATED STAINLESS STEEL LIQUID HEAT EXCHANGER
6	3	THERMAL SWITCH, MODEL 3100
7	1	LASER
8	1	DE-IONIZATION FILTER
9	1	PRIMARY COOLANT PUMP
10	2	COOLANT RESERVOIR
11	2	TEMPERATURE SENSORS
12	2	HEX HEAD PLUG 1/4" NPT
13	2 (SETS)	QUICK DISCONNECT 3/8"
14	6 (SETS)	QUICK DISCONNECT 1/2"
15	4	TEMPERATURE MONITOR
16	1	25 WATT HEATER
17	1	25 WATT STRIP HEATER

again turned on.

3.6 Payload Electronics

The ABLE payload electronics were implemented primarily with a CAMAC (Computer Automatic Measurement And Control) system. The functions of system are as follows:

- 1) Lidar data acquisition
- 2) Housekeeping data acquisition
- 3) Data formatting and PCM Bi -L encoding
- 4) Uplink modem command decode
- 5) System timing
- 6) Pointing mirror control
- 7) HG tuning control
- 8) Temperature monitor and control

Figure 15 is a block diagram of the payload electronics. The lidar detector data flow is shown in Figure 16. The real-time data processing was outlined in the R & D Design Evaluation Report. The lidar data format and physical conversion factors were presented in the ABLE Interface Control Document.

3.6.1 Payload Power

The primary power source of the lidar experiment payload is government-furnished Ag-Zn batteries. These batteries are nominally rated at 80 amps-hrs capacity and at 1.5 volts/cell. They are packaged in polystyrene containers to maintain the battery temperature at approximately 20°C throughout the flight. Each battery container consists of two 20-cell batteries. Of these, 18 are series connected to provide a nominal 27 Vdc power supply. The specified voltage range for these batteries is 28 ± 4 Vdc. Each battery has provision for charging. The entire payload can be operated during test under external power by the use of laboratory power supplies.

The laser power batteries are dedicated solely to laser operation to minimize system RFI/EMI. The number of batteries required for laser operation is dependent on the specified number of hours of continuous operation. These multiple laser batteries were connected in parallel with steering diodes used to prevent cross coupling (i.e. current from one battery going into another as a result of a lower voltage). Visidyne used its flight-tested power system design for the lidar experiment. Two batteries were used for the receiver and one each for the thermal control system and housekeeping.

3.6.2 Telemetry

The ABLE payload downlink telemetry system used two PCM links which are designated as the lidar data link and the balloon data link. The lidar data

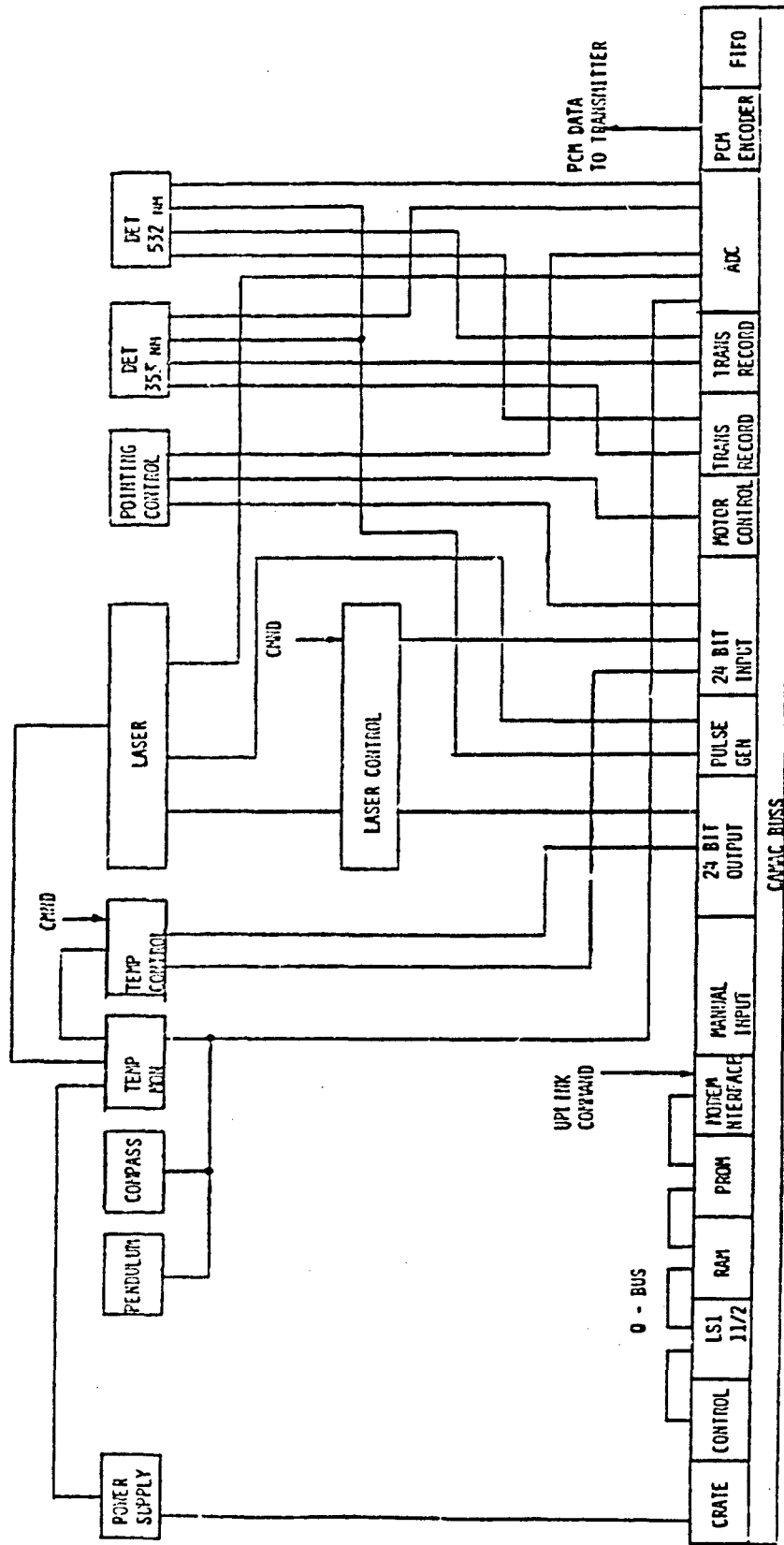


Figure 15. ABLE Payload Electronics, Block Diagram

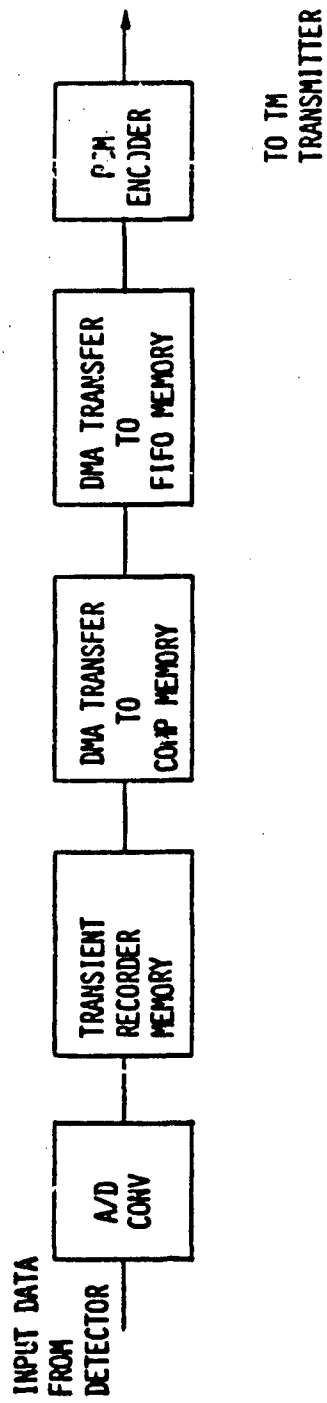


Figure 16. Lidar Detector Data Flow

link transmits data for the 355 nm and 532 nm receivers and payload housekeeping data.

Universal time is melded with data when it is recorded at the ground station. These data are combined with the specified PCM synchronization bits as per IRIG 106-80, converted to a serial bit stream, converted to a Bi-L format and fed to the payload telemetry transmitter. Visidyne, Inc. designed, fabricated, and tested the PCM encoder for the lidar data.

3.6.3 Payload Orientation System

As a heading reference, the balloonborne lidar payload uses a simple compass, the Model 101 Marine Heading Sensor made by DigiCourse, Inc. This sensor is an optoelectronically-read magnetic compass that transmits heading information via a five-conductor cable to a Model 250 Interface Unit. The internal gimbaling accommodates plus or minus 70 degrees in pitch and roll. The binnacle contains compensation magnets mounted at each end of two plated brass rods that run at 90 degrees to each other across the binnacle near the bottom.

The payload angle relative to the local vertical is determined by two axis data provided by two pendulums located in the CAMAC electronics chamber.

3.7 Data and Command Software

The software developed for ABLE was developed to perform the following functions:

1. CAMAC electronics control
2. lidar detector data acquisition
3. housekeeping data acquisition
4. pointing mirror control
5. digital data I/O
6. experiment timing
7. IRIG PCM data encoding
8. modem command control
9. CAMAC module task
10. ground support programs which provide tabular and graphical output of lidar data in real time.

Detailed descriptions of the data system operation and the data format were given in the R and D Design Evaluation and The ABLE Interface Control Document respectively.

4. SAFETY CONSIDERATIONS

4.1 Introduction

In the earlier design phase of ABLE experiment,^[2] Visidyne considered rigorously and in detail the safety precautions to be taken due to laser radiation and high voltage involved. In this document, for the sake of brevity and because they are still valid, we will in general summarize the previous work.

4.2 Laboratory Safety

Two principal types of hazards are associated with laser operation: the laser radiation itself and the high voltages present in the laser power supply. Few serious injuries due to lasers have been reported since the introduction of commercial models. The accident rate has been low because the possibility of exposure of the eye to a collimated beam is extremely remote if a few basic precautions are followed. On the other hand, electrical hazards have proved to be far more serious, and a number of guidelines should be followed to prevent electric shock.

The problem of protective eyewear was compounded by the three radiation wavelengths of the neodymium:YAG laser at 1064, 532, and 355 nm. However, it was readily solved by combining two broad spectrum filters, from Glendale Optical Co., designed for neodymium frequency-doubled lasers. The luminous transmittance of this combination was 20%, which was more than adequate for laboratory work, while the minimum optical density at the laser wavelengths was 8.

During the performance of the laboratory phase of the program, the guidelines and precautions set forth for protection from laser radiation and electric shock were rigidly adhered to by all personnel, and the work was completed without incident.

4.3 Range Safety Requirements

Operation of the laser in the field prior to launch or after payload recovery requires guidelines as given above for use in the laboratory. However, once the payload is aloft, the possibility arises that the laser radiation may be viewed by someone not using protective eyewear. The standards for the use of lasers, such as those set by the American National Standard Institute(ANSI)^[5] and which are usually adopted or modified by BRH and OSHA, define the permissible exposure limits.

In connection with the field operation of the ABLE system, the AFGL project scientist prepared an environmental assessment. This document examines in

quantitative detail the potential dangers associated with the operation of the balloonborne ABLE payload. In Reference 2, we had previously determined that for eye range safety, the principal danger is from the pulsed 532 nm laser radiation, and that by comparison, the danger from the other two laser wavelengths is unimportant. The environmental assessment document considers the rare, but possible, worst case of an accidental observer located within the laser-illuminated ground area who might train 7x50 binoculars on the balloonborne ABLE lidar source at float altitude. This case would exceed the Maximum Permissible Exposure value. Consequently, to ease the eye safety problem, the divergence of the laser output beam was increased from 1 to 2 mrad by the addition of a long focal length negative lens in the transmitter beam.

Firing of the laser in the field was always rigorously controlled. For ground testing, the arm and fire commands could not be initiated until two individuals activated two key switches on the payload control panel. Laser firing after launch was at all times under direct command from the ground, and was controlled by several separate and independent methods, as follows:

1. Laser firing was enabled only when uplink commands of laser POWER ON (OFF), laser ARM (DISARM), and laser FIRE (INHIBIT) were transmitted. Any interruption in continuous receipt of the FIRE command would terminate firing.
2. A similar, redundant command system also controlled laser firing and the pulse repetition rate.
3. A barometric pressure switch was preset to inhibit any laser firing at payload altitudes below 15 kft.
4. Interlock switches inhibited any laser firing when the pointing mirror was moving or in the stow position.
5. A payload-mounted clock timer was preset to terminate any laser firing eight hours after launch.

Directional firing of the laser during flight was controlled as follows:

1. Horizontal firing: all beam energy directed into a payload-mounted energy dump.
2. Upward firing: limited to payload altitudes above 30 kft.
3. Downward firing: limited to only when the payload was at float altitude (above 60 kft) and over the approved regions of the White Sands Missile Range.

The environmental assessment document also noted that the lidar beam presented no hazard to wild life, and that no toxic materials would be released during the balloon operations, which, moreover, were identical to those of many previous flights.

5. TEST, CALIBRATION, AND ALIGNMENT

As part of the contractual work statement, in January 1983 Visidyne published an R and D Test and Acceptance Plan. This document listed all testing of the ABLE system and subsystems proposed as of the date of its publication. The actual testing, reported below, modified somewhat and improved on the proposed testing. The thermo-vacuum and other tests that were conducted in the field are discussed as part of the field operations.

5.1 Transmitter Tests

Testing of the government-furnished International Laser Systems Nd:YAG laser was conducted principally at the Air Force Geophysics Laboratory. These tests were designed to verify and compliment the manufacturer's test data. These tests included the following:

1. Proper operating procedures
2. Crystal tuning procedures
3. Laser energy calibration
4. Beam divergence measurements
 - a. At a distance
 - b. focused with long focal length lens
5. Beam waveshape

The laser energy monitor was tested and adjusted to assure that it would give accurate measurements of the laser output at all three wavelengths.

The above tests were made using EG and G and Scientech radiometers with appropriate combinations of filter glasses, dichroic beam splitters, apertures, and other optical components.

5.2 Receiver Tests

The receiver telescope optics were mounted in the telescope baffle assembly by the manufacturer, and focusing tests were witnessed by Visidyne personnel. No further focusing adjustments were made. The reflectivity of the mirrors was checked with a witness sample which was coated at the same time as the telescope mirrors.

The spectral transmission of the oven-controlled, narrowband filters was checked at their operating temperatures by an independent source and witnessed

by Visidyne personnel. The receiver was checked for any possible vignetting of the field of view.

5.3 Pointing System Tests

The laser pointing mirror initially was constructed with the same substrate and coating as the telescope mirrors. However, when tested for laser-induced damage with the ILS laser, the mirror coating was severely affected. Consequently, the mirror was replaced with one having a multilayer dielectric coating on a glass substrate. Subsequent tests with the ILS laser caused no damage to this mirror, and the pointing system mount was modified to accommodate it.

Alignment of the two pointing mirrors was done using an autocollimator and an alignment device containing two plane mirrors mounted parallel to each other a meter apart on a rigid beam. This device and its use are discussed more fully in Section 5.5.1.

The pointing mirror drive mechanism was tested using the CAMAC electronics for proper positioning, slew rate, backlash, and angle monitoring by an optical encoder.

5.4 Thermal Control System Tests

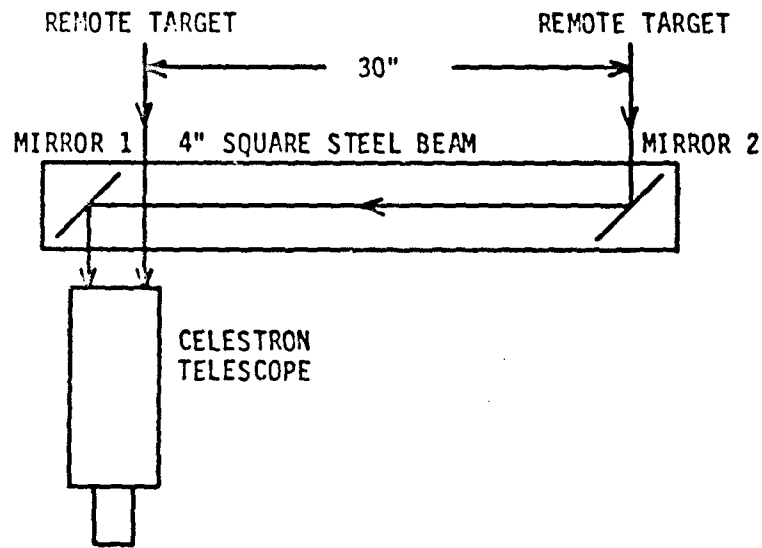
The assembled thermal control system was pressure and leak checked, and the coolant flow rate was checked. However, the principal test of the system was during the thermo-vac chamber test conducted as part of the field operations. This test is discussed in detail in Section 6.2.

5.5 System Testing

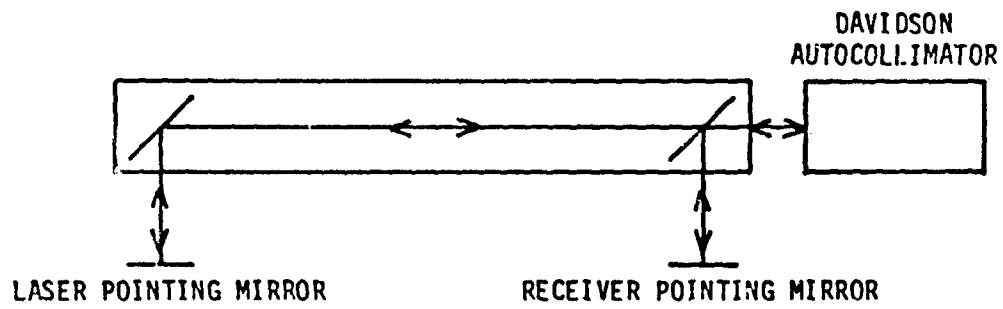
5.5.1 Optical Alignment

Optical alignment of the pointing mirrors and the lidar system was simplified through the use of a unique optical bench shown in Figure 17. We installed two mirrors on adjustable mounts separated by 30" in a 4" square structural steel beam in which we had cut appropriate ports. The mirrors have protective aluminum coatings on clear, plane-parallel substrates so that they could be used as either first or second surface mirrors. The two mirrors were adjusted parallel to each other by the method shown in Figure 17.a. Using a 4" Celestron telescope focused on a distant (many miles) target, the mirrors were adjusted and set so that the direct image and the mirror-deflected image of the target were coincident. The possible error in this alignment procedure was estimated to be 0.02 mr.

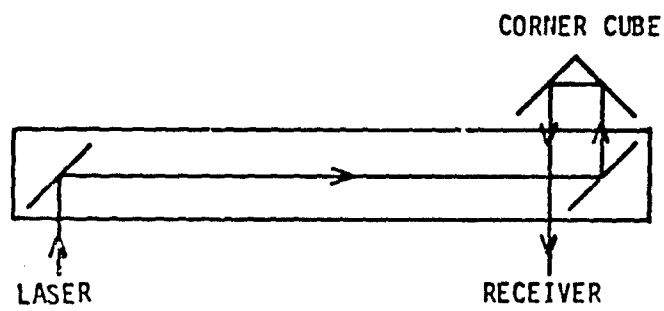
The method for aligning the pointing mirrors is shown in Figure 17.b. The pointing mirror shaft was rotated until the two pointing mirrors were re-



a) Optical Beam Alignment



b) Pointing Mirror Alignment



c) Lidar System Alignment

Figure 17. Optical Alignment Methods

flecting away from the payload. Using a Davidson autocollimator, the reticle pattern reflected from the laser pointing mirror was made coincident with the reticle pattern reflected from the receiver pointing mirror by adjusting the mounting of the former. Both reflected beams could be seen in the autocollimator because Mirror 2 is shorter than Mirror 1.

The optical alignment adjustments of the lidar system are shown in Figure 18. In preparation for aligning the lidar system, an eyesafe He-Ne laser beam was made coincident with the Nd:YAG laser beam. To facilitate this procedure, a port having a transparent plexiglass cover was included in the design of the Nd:YAG laser pressure chamber. The He-Ne laser was directed at the polarizer shown in Figure 6 and oriented so that a transmitted portion of its beam could be observed at the lidar laser output. Then by alternately firing the Nd:YAG laser and adjusting the position of the He-Ne laser, the two beams were made coincident as determined by noting their locations on a remote surface. Next, the optical bench, with the addition of a corner cube reflector, was set up in front of the lidar system as shown in Figure 17.c. At the receiver telescope focus, we installed a translucent screen with concentric rings calibrated in milliradians. With the He-Ne laser, the beam was centered on the screen by using the optical axis alignment system shown in Figure 18. Finally, the alignment was checked by firing the Nd:YAG (strongly attenuated by filters) and photographing the position of the 532 radiation on the screen. The estimated alignment accuracy of the lidar system by this method was 1 mr.

5.5.2 Lidar Calibration

The laser transmitter output was calibrated as described in Section 5.1. Two independent methods were used to calibrate the receiver. In the first, a calibrated tungsten ribbon lamp was used in combination with a small aperture and a collimating lens positioned so that all radiation from the aperture would be incident on the receiver telescope optics and pass through the telescope field stop aperture. Appropriate values as given in Table 3 for transmission, reflection, and spectral bandwidth of the receiver components were employed together with the appropriate responses of the photomultiplier detectors.

In the second method, a standard irradiance, coiled filament lamp was used to illuminate, at a prescribed distance, a large Lambertian surface mounted in front of the receiver telescope. The telescope collecting area was apertured down to a 10x10 cm opening. Optically then, the telescope appeared to be view-

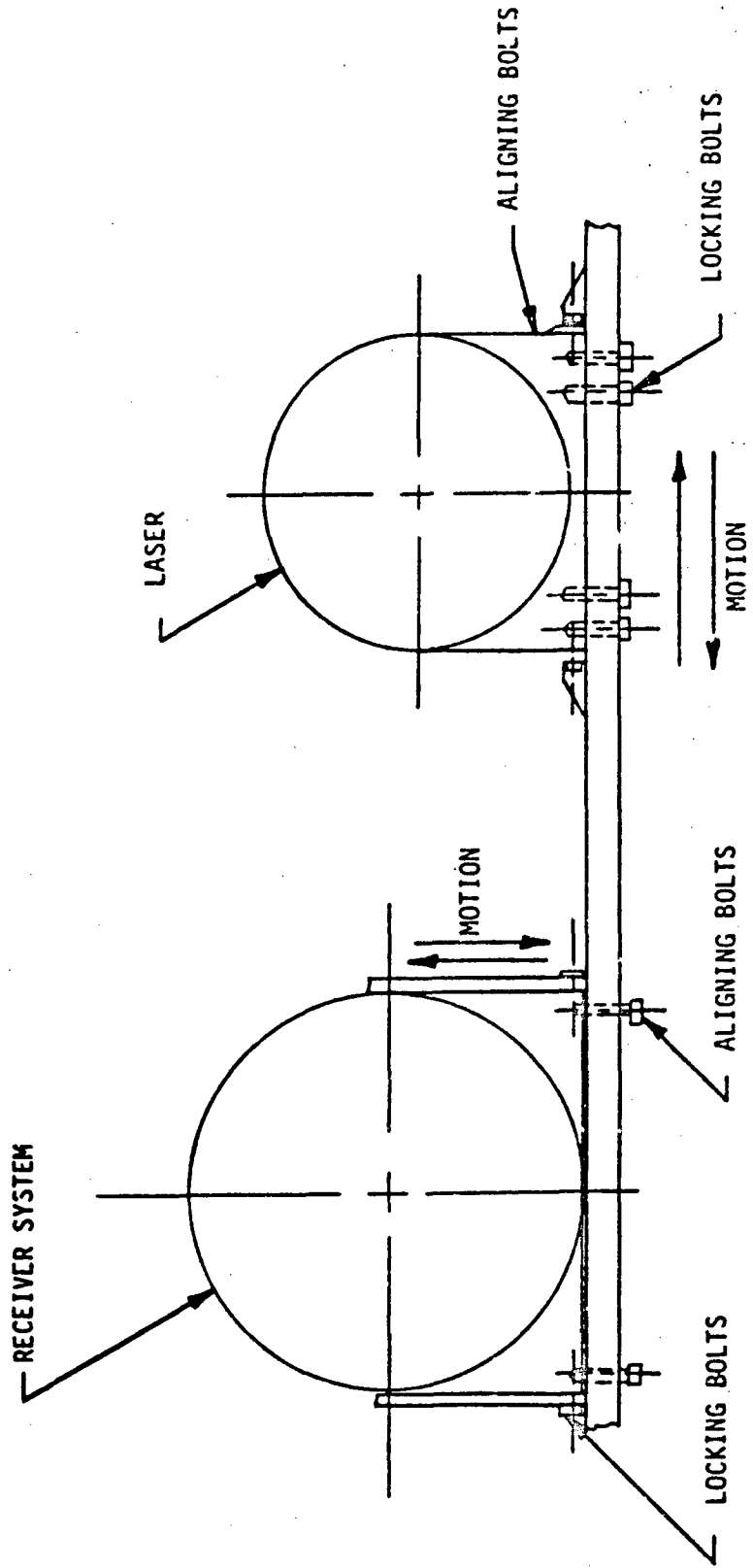


Figure 18. Optical Axis Alignment System

ing, with a known aperture, an extended source of known irradiance. Other factors were as in the first method. Results of the two methods were then compared.

5.6 Environmental Tests

The object of the environment tests was to subject the payload as close as possible to simulated conditions of launch, ascent, and float. Table 7 lists the payload environment design specifications with respect to temperature, pressure, and mechanical shock.

5.6.1 Pressure Vessel Test

Pressure tests were performed on the pressure chambers prior to their acceptance. For these tests, the chambers were assembled and tested as a unit. The following tests were made:

1. Perform proof test to 30 psi differential.
2. Pressurize with air to 15 psi differential and inspect for leaks using a bubble solution.
3. Pressurize with air to 15 psig and monitor pressure and temperature. Pressure loss after 48 hours shall not exceed 2 psi after temperature correction .

After assembly of the instrumentation in the chamber, Test Number 3 was repeated as necessary.

5.6.2 Shock Test

Evaluations of previous balloon payload launches had indicated that shock levels up to two g's may be encountered at launch. This was on payload release from the crane and occurred only if the balloon load lines and payload were not lined up at the moment of crane release. The ABLE payload was tested for launch shock loads of two g's. This was done by dropping the payload a calibrated distance and recording g levels on various critical parts of the payload.

5.6.3 Thermovac Test

The thermovac test simulates ambient conditions predicted to be encountered by the payload during ascent to about 30 km and float at that altitude for about six hours. Thermovac testing was to have been performed at the facility at AVCO Wilmington prior to field operation. However, the compressor pumps at the AVCO facility had failed and could not be replaced in time, so that thermovac testing of the ABLE payload was performed at Holloman AFB as part of the field operations. Details of the test are given in Section 6.2.

Table 7. PAYLOAD ENVIRONMENTAL SPECIFICATIONS

<u>EVENT</u>	<u>DEFINITION</u>	<u>COMMENTS</u>
TEMPERATURE		
PRELAUNCH	5 TO 35°C	OPERATIONAL
BALLOON ASCENT	-71°C MINIMUM	AMBIENT AIR TEMPERATURE
	25 ± 5°C	DESIGN GOAL, REQUIRED FOR LASER AND RECEIVER
	10 TO 35°C	OPERATIONAL ELECTRONICS TEMPERATURE
BALLOON FLOAT	-46 TO -20°C	AMBIENT AIR TEMPERATURE
	25 ± 5°C	DESIGN GOAL, REQUIRED FOR LASER AND RECEIVER
	10 to 35°C	OPERATIONAL ELECTRONICS TEMPERATURE
PRESSURE		
PRELAUNCH	14.7 ± 4 PSI	
BALLOON ASCENT	14.7 TO 0.029 PSIA	AMBIENT PRESSURE CHANGE WITH ALTITUDE
BALLOON FLIGHT	0.16 TO 0.029 PSIA (FOR UP TO 12 HRS)	FLOAT ALTITUDES FROM 100,000 TO 140,000 FEET
MECHANICAL SHOCK		
LAUNCH	2 G, 70 MSEC, HALF SINE ALL AXES	NO DEGRADATION OF EXPERIMENT SYSTEM PERFORMANCE
CHUTE OPENING	10 G, 70 MSEC, HALF SINE ALL AXES	LASER IS NOT REQUIRED TO MAINTAIN ALIGNMENT. NO PERMANENT DAMAGE IS PERMITTED. OPTICAL MISALIGNMENT IS PERMITTED.
GROUND IMPACT	CAN BE >10 G IN Z	AMOUNT OF DAMAGE WILL DEPEND ON TERRAIN, HORIZONTAL IMPACT, VELOCITY, AND SECOND IMPACT

6. FIELD OPERATIONS

6.1 Scenario

Figure 19 shows the geographical region of the ABLE field operations. The requirement for low background levels in the two wavelengths of interest dictated that the data be taken during a night flight. Thus the balloon launch was scheduled for around sunset. The selection of a launch time depended upon both the low level ground wind conditions, wind shear, and high altitude winds. It was desirable to keep the payload flight path over the controlled airspace of White Sands Missile Range (WSMR) for as much of the flight as possible. As long as the payload was over the controlled airspace, the lidar could be directed downward since this provides the most complete density distribution data.

Launching the payload from Holloman AFB and having the lidar system over the restricted area of WSMR when float altitude is reached is highly improbable. This is due to the time it takes to reach float altitude and wind effects on the balloon during ascent. Also, the predictability of the wind velocity at 100,000 feet during the "turnaround" period (winds light and variable, 0-5 knots), is only ± 10 knots. In other words, although the wind at 100,000 feet might be predicted to be from the west at 5 knots, when the payload reached float altitude, the wind might be from the east at 5 knots. Launch should take place when the winds at 100,000 feet are predicted to be 15-20 knots since upper atmospheric winds of at least this speed are quite steady and predictable.

For the above reasons, it was first suggested that the lidar payload be launched from an area near Truth or Consequences, New Mexico, which is about twenty miles to the west of the western edge of WSMR. This would enable the payload to reach operational altitude while still over the restricted area of WSMR as shown in Figure 19. However, a survey of the available facilities at Truth or Consequences revealed that they were far from adequate.

Consequently, the decision was made to conduct the launch operations from the Roswell Industrial Air Center, where many previous balloon launches had been made. The time of year chosen for ABLE launch was August when the winds are easterly. The only disadvantage was that launch would now be over 60 miles to the east of the eastern edge of WSMR, so that the lidar could be directed downward only much later in the flight. This could have been a problem if the balloon flight path were to drift away from a nearly westerly direction, or if the lidar system were to experience some unexpected degradation as the flight progressed.

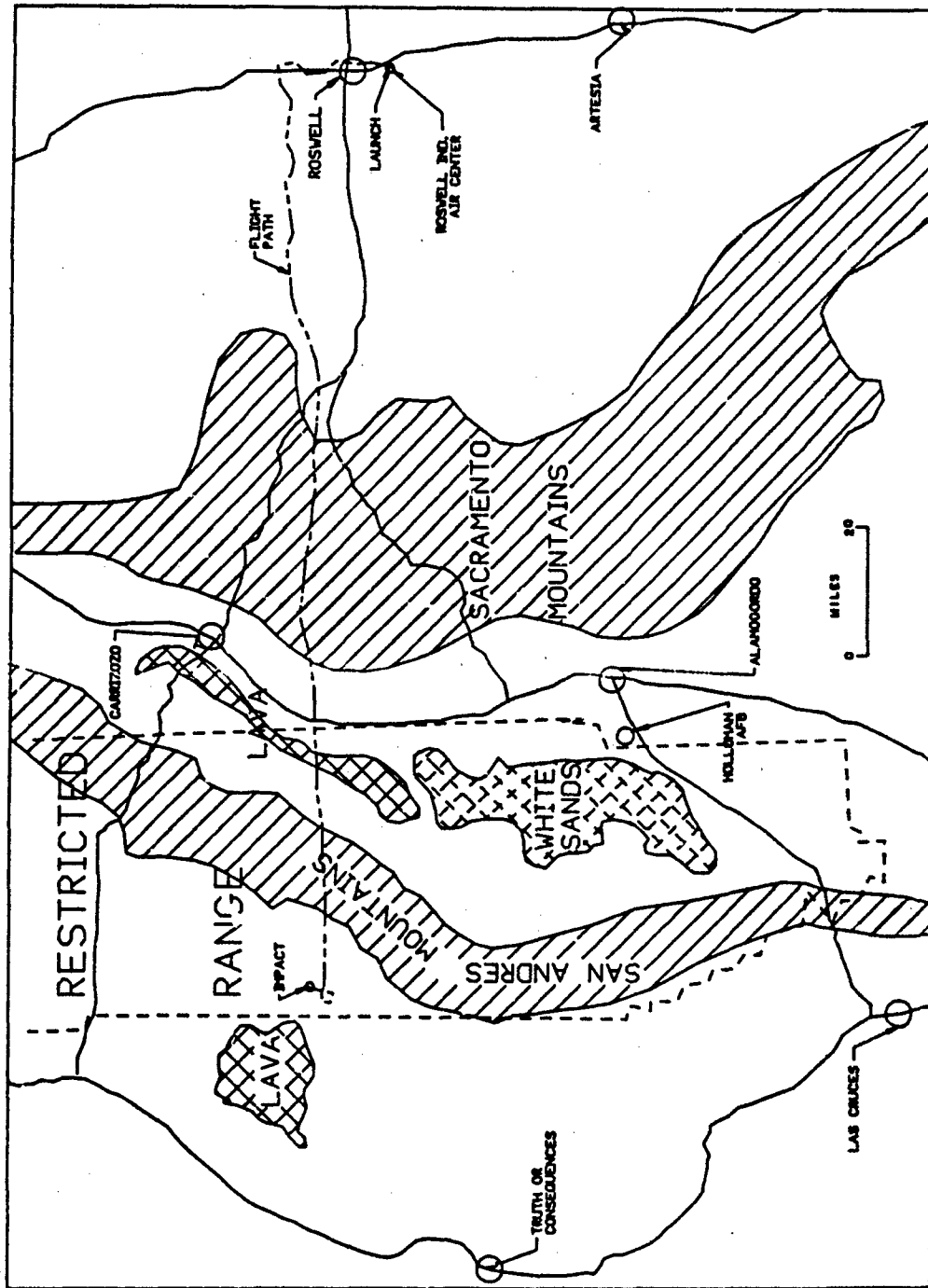


Figure 19. Site of ABLE 1984 Field Operations

Having made the decision to launch from Roswell, NM, the contract personnel devised the launch schedule for ABLE listed in Table 8. This schedule was followed closely during the actual field operations, as we shall note in the sections that follow.

6.2 Thermovac Test

6.2.1 Test Setup and Procedures

The thermal-vacuum (thermovac) testing of the ABLE payload was performed in the Stratosphere Chamber located at Holloman AFB. Figure 20 shows the payload set up in the chamber. Specifications of the chamber are listed in Table 9. The planned test profile was as follows:

1. Altitude rise for 65 minutes at 800 ft/min to 52,000 ft and -70°C . Cooling to begin only after chamber at 16,000 ft to remove moisture.
2. Hold for 30 minutes.
3. Altitude rise for 65 minutes at 800 ft/min to 104,000 ft and -40°C .
4. Hold for 150 minutes.
5. Conclude test by venting chamber to 50,000 ft and turning on infrared lamps to heat payload. Then turn on electrical heaters to heat air to ambient temperature and vent chamber to ambient pressure.
6. Leave payload in chamber overnight.

For the test, optical components were set up in the chamber so that the laser beam could be viewed in the chamber anteroom during testing for possible orientation or quality changes. The protective covers were left on the receiver optics to help prevent any contamination resulting from the test procedures.

6.2.2 Test Results

The actual profiles of the chamber altitude and temperature during the test are shown in Figure 21. Both the temperature and altitude extremes were somewhat more severe than planned. Nevertheless, the ABLE payload performed quite well. The pointing system movement was unaffected; the laser firing showed no ill affects and the beam remained steady. The radiational cooling appeared to be more than originally calculated. As a result, prior to launch, additional insulation was added to the various payload chambers, and one third

TABLE 8. ABLE LAUNCH SCHEDULE-1984

DATE	WEEKDAY	TASK
Aug. 3	FRI	Travel
Aug. 4	SAT	Unload and unpack payload and support equipment at Bldg 850, Holloman AFB
Aug. 5	SUN	Payload inspection
Aug. 6	MON	Payload test, optical alignment, pressure test
Aug. 7	TUE	Payload test, TM up
Aug. 8	WED	Payload into thermal vac chamber, Bldg 850 TM test, external power, Bldg 850 TM test, internal power
Aug. 9	THU	Thermovac test
Aug. 10	FRI	Remove payloads from chamber. Pack
Aug. 11	SAT	Open
Aug. 12	SUN	Open
Aug. 13	MON	Ship payload to Roswell Industrial Air Center. Unpack
Aug. 14	TUE	Payload test, alignment, and pressure test
Aug. 15	WED	Payload test, calibration
Aug. 16	THU	All-up payload test, external power, TM van
Aug. 17	FRI	TM test tape to Bldg 850
Aug. 18	SAT	Open
Aug. 19	SUN	Open
Aug. 20	MON	L-3 test, internal power, TM van
Aug. 21	TUE	Compass calibration, lidar calibration
Aug. 22	WED	Final battery charging
Aug. 23 Aug. 28	THU to TUE	LAUNCH WINDOW
Aug. 29	WED	Payload recovery
Aug. 30	THU	Pack
Aug. 31	FRI	Travel

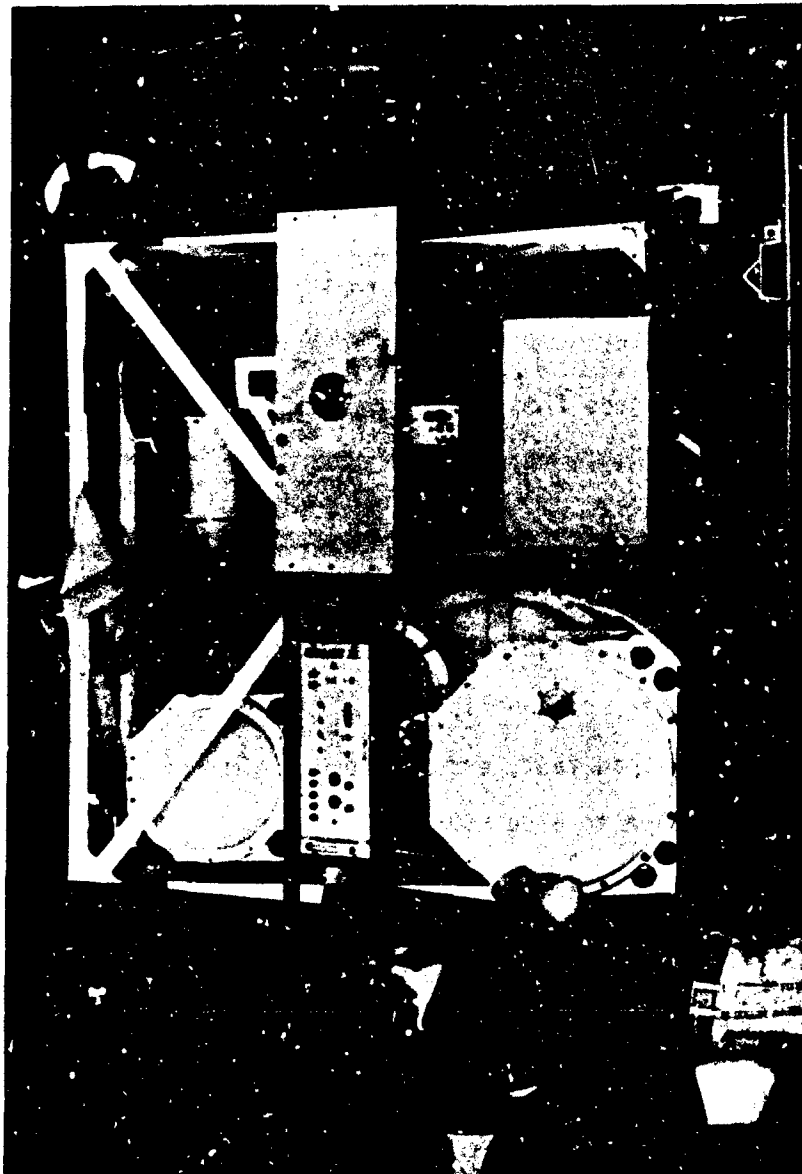


Figure 20. ABLE Payload Set Up for Thermovac Test

TABLE 9. STRATOSPHERE CHAMBER SPECIFICATIONS

SPECIAL FEATURES: Designed to create controlled and combinable conditions of altitude, humidity, infrared radiation, and vibration in a laboratory room. The unique part of this chamber's operation is its rates of change, and the ability to program the environmental variables automatically and independently, or simultaneously. These variables can be programmed for extended periods of "flight" time—for example, 48 hours.

ALTITUDE: 140,000 feet in 4 minutes: 220,000 feet approximate ultimate.

AIR TEMPERATURE: -100°F To +200°F (Dry Bulb)

HUMIDITY: 15 to 95% RH at 35 to 140°F. Dew points of -50°F possible by use of an air drying system.

TEST SPACE SIZE: Chamber: 8' wide x 8' high x 11' long
Anteroom: 4' wide x 4' long

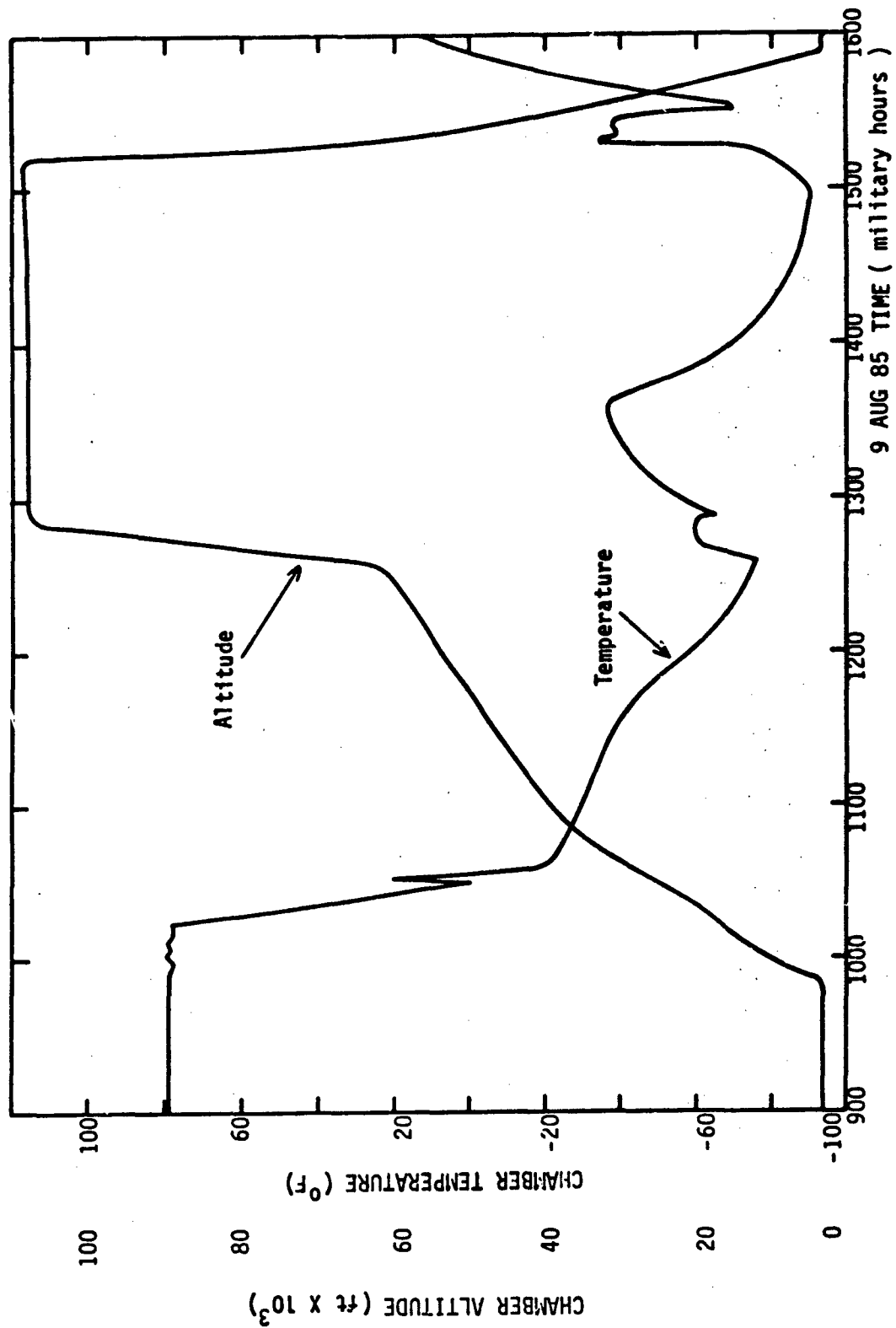


Figure 21. Thermovac Chamber Altitude and Temperature during ABLE Payload Test.

of each of the two radiator panels was covered with insulation. The ultraviolet detector chamber lost pressure during the test due to a leaky connector seal. This caused a failure of the photomultiplier tube high voltage power supply. After the test, the cause of the leak was found and remedied, and the power supply was replaced.

A failure of the CAMAC crate controller occurred after completion of the thermovac test, probably when the payload was cold-soaked while the chamber was allowed to warm up slowly overnight. A replacement controller was obtained for payload testing and the flight unit repaired in time for the prelaunch test. Other than the above, the thermovac test served principally to confirm that the ABLE payload has been correctly designed and properly fabricated for lidar measurements from the upper atmosphere.

7. FLIGHT OPERATIONS

Upon completion of the thermovac test at HAFB, the payload and support equipment were packed and trucked to the Roswell Industrial Air Center. Here the payload was unpacked and set up for the final tests and preparation for launch. The ABLE launch and flight operational procedures are in Appendixes C through J .

7.1 System Tests

Prior to launch the following system tests were performed:

- 1) Battery charging and testing
- 2) Chamber pressure tests
- 3) Laser/LEM calibration,(Figure 22)
- 4) Payload EMI testing
- 5) Payload telemetry test
- 6) All up test at L-3 days

7.2 Flight Summary

On August 23, 1984 at 2130 hr local time, the Atmospheric Balloon Lidar Experiment, ABLE payload was launched from Roswell, New Mexico. The payload attained an altitude of 107,000 ft approximately 3 hours after launch. The lidar experiment was operated successfully at altitudes greater than 60,000 ft as per the experiment plan. The objectives of the flight were to provide an experiment test of a balloonborne lidar and to make atmospheric backscatter measurements with 150 meter slant range resolution using a lidar system. Both objectives were successfully met. The purpose of this section is to discuss the flight and the lidar system operation.

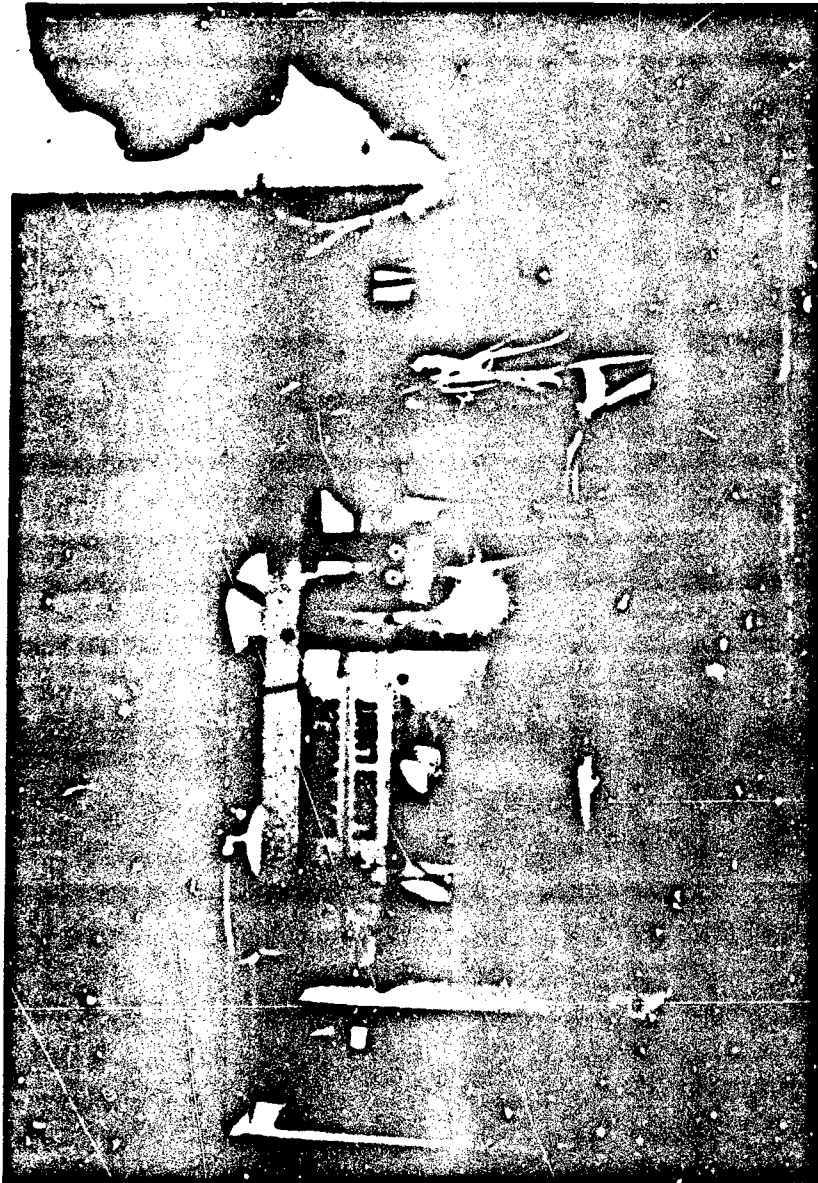


Figure 22. Laser/LEM Calibration Test

ABLE launch was first scheduled for 2000 hours on August 23, 1984 when acceptable weather conditions were predicted at the Roswell Industrial Air Center launch site. These conditions were as follows:

- 1) Absence of thunderstorm activity at the launch site
- 2) Absence of thunderstorm activity at the recovery site at the time of termination
- 3) Low surface winds at the launch site

Local thunderstorm activity delayed the rollout of the payload to the launch area from the scheduled 1600 hours to 1730 hours. The payload was enclosed in an electrically-conductive plastic covering to protect it from dust accumulation during the short (100 yd) required transit over a dirt road to the runway. Upon arrival at the launch area, the payload covering was stripped off. Payload instrument checks (Appendix G) were commenced at about 1800 hours. It was required to repeat the test sequence because a faulty reel of tape prevented the recording of the initial test data. The ABLE test data were reviewed, and it was concluded that the payload was ready for flight.

The next step in the launch countdown, balloon layout, was delayed because of local thunderstorm activity. It was estimated that a storm was within 7 miles of the launch area so the payload was again bagged. At 2030 hours it was concluded that the local thunderstorm danger had abated and that there was a high probability that the present thunderstorm activity at the predicted recovery site would abate prior to the time of termination. The decision, coordinated with the project scientist at HAFB Bldg. 850, was made to launch, and balloon layout was initiated. The payload cover was removed and the payload was put into a launch condition, (reference Appendix H). Figure 23 shows the payload and the inflated balloon prior to release. At L-15 minutes the payload was powered up per Appendix H. At 2132 hours the ABLE payload was launched without being subjected to any apparent mechanical shocks.

Shortly after launch, it was found that the balloon control system was unable to dump ballast. This resulted in a slower rate of ascent than planned, thus subjecting the payload to cold soaking longer than normally would have been encountered. The implications of this are discussed further in Section 7.2.5.

During ascent, telemetry dropouts occurred at the Roswell site. This may have been caused by interruption of the telemetry antenna line-of-sight by the hangar structure and power transformer.

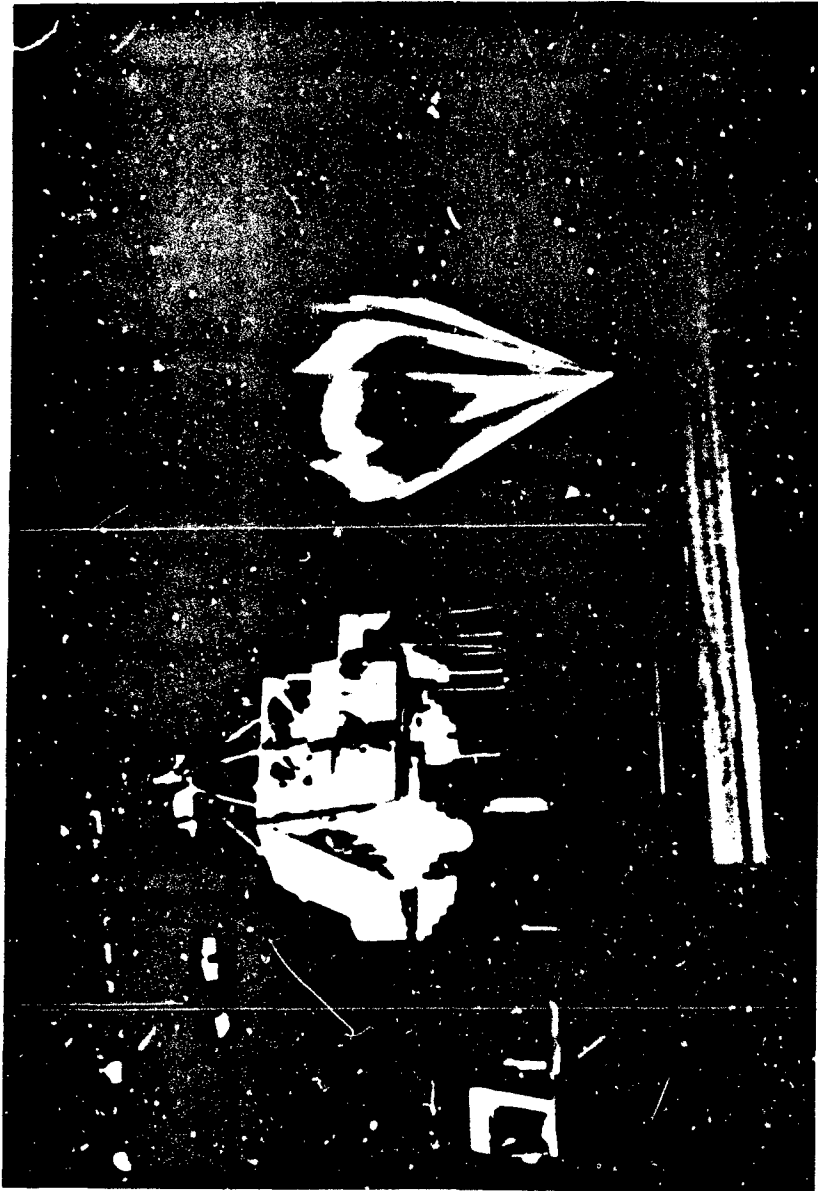


Figure 23. ABLE Payload and Balloon prior to Launch

At about 2230 hours, control of the payload and data recording/monitoring responsibility were transferred, as planned, to Bldg. 850, Holloman AFB. This transfer concluded the launch operation.

During the flight, the ABLE lidar system operated successfully, and excellent backscatter data were acquired.

7.2.1 Laser

The ABLE laser was operated on command throughout the flight, and relatively stable radiant output energies were obtained of the three laser output wavelengths, 1064 nm, 532 nm, and 355 nm. The laser operated in an air temperature of typically -12°C , and the laser power supply air temperature was -3°C during the latter part of the flight. Although the laser operated acceptably in this low temperature environment, it is recommended that the laser thermal system be modified to maintain the laser operation temperature range to within 10 to 30°C .

The laser SHG and THG crystals could be angle-tuned by the uplink command system (reference 2). This tuning system was not fully tested until after deployment into the field. During payload testing at Roswell, it was found that one axis of each crystal was incorrectly assigned to the other crystal, resulting in a detuning of the harmonic generator. This problem was corrected by modification of the tuning command definition. It is recommended that the crystal tuning drives be replaced with drives having optical encoders, thus permitting the absolute position of each crystal axis to be monitored.

The harmonic generator tuning was not used during the flight because of the limited amount of experiment time over the range, but it was successfully tested during the preflight laser testing.

7.2.2 Laser Energy Monitor (LEM)

During lidar testing the UV LEM data was considerably more noisy than the RED or GREEN data. It was concluded that an accurate measurement of the UV laser energy output could be made by measuring the peak value of the LEM output.

During the flight, an increase in the noise of the RED and GREEN LEM data was observed. This noise increase may have been caused by the low temperature (-10°C) at which the LEM was operating during the flight. It is recommended that the LEM be subjected to testing to determine the cause of the observed noise and then modified to correct this problem.

7.2.3 Receiver

The lidar receiver operated as specified throughout the flight. From a preliminary inspection of the flight lidar data, it has been concluded that the laser optical axis and the receiver optical axis remained coaligned throughout the flight. The pointing mirror operated as per specifications during the flight.

The optical filters in the receiver were designed to be maintained at a constant elevated temperature to maintain the peak transmission wavelength of the filter. During the flight the filter temperature dropped to -10°C for the UV filter and -20°C for the GRN filter. It has been determined that the laser line transmissions were not seriously degraded by this temperature change. It is recommended that the filter insulation be increased for the next flight.

The receiver detectors were operational throughout the flight, although the initial quick-look data indicated incorrectly that the GRN detector was not operational. This was probably caused by a malfunction of the ground-based, quick-look data system software.

Some low-amplitude, high-frequency noise spikes were present in the detector data. This noise was not correlated with laser firing, and thus can be averaged out by either averaging over a number of shots for each range bin or by a running average over several range bins for each shot. It is recommended that the cause of this noise be determined and corrective action taken.

7.2.4 Data and Command

The onboard data and command system, which utilized the CAMAC electronics, operated flawlessly throughout the flight. Some telemetry dropouts which occurred early in the flight were probably caused by poor antenna payload aspect. The uplink modem command system functioned reliably during the flight with no false or spurious commands being observed. The discreet tone command system was operated with the same reliable results.

7.2.5 Thermal Control

The payload thermal control system was operational throughout the flight, but some thermal problems were encountered. These were the following:

- 1) The coolant circulation flow in the secondary coolant loop was greatly reduced by the low temperatures encountered during the flight. It should be noted that these temperatures were lower than the design environmental specifications of the R and D Design Evaluation Report.

- 2) The internal temperature of the laser chamber and the laser power supply chamber were not maintained in the specified temperature range.

It should be noted that the thermal control system for the CAMAC electronics chamber operated throughout the flight so as to maintain the chamber internal temperature within the specified range of 10 to 35°C.

7.2.6 Payload

The payload, including structure, batteries, and interconnecting cabling, functioned properly during the flight. All five hermetically-sealed chambers maintained pressure during the flight. The seven Ag-Zn batteries maintained full 28 Vdc throughout the flight.

During the recovery operations of termination, parachute opening, and ground impact, the payload accelerometer never sensed more than one g in any axis. Minor bending of several outrigger structural members occurred, probably due to the full ballast hoppers, not a normal termination condition.

7.3 Payload Recovery

The flight time was terminated to bring the payload down within the White Sands Missile Range. The morning following the flight, a recovery crew, including four project experiment personnel, left Building 850 to locate and recover the payload.

The payload was located by aircraft and the recovery crew was guided to the payload. The payload was found adjacent to a dirt road, as shown in Figure 24. It was approached first by the eye-protected experiment crew. This crew initially safety interlocked the laser and turned off all electrical power on the payload. Next the receiver and transmitter optics were covered. When it was concluded that the payload was in a safe condition, the Detachment 1 recovery crew was permitted to approach the payload and start the loading process. The payload was loaded onto mattresses on the flatbed trailer using the DST crane. The payload was then trucked back to Building 850. Here the payload was off-loaded, inspected, tested, and packed for redeployment back to Visidyne, Inc.

7.4 Quick Look Data

The flight PCM data was decoded in real time and the housekeeping data displayed on a CRT terminal. Approximately each 15 minutes, a full hard copy of the data was printed out.

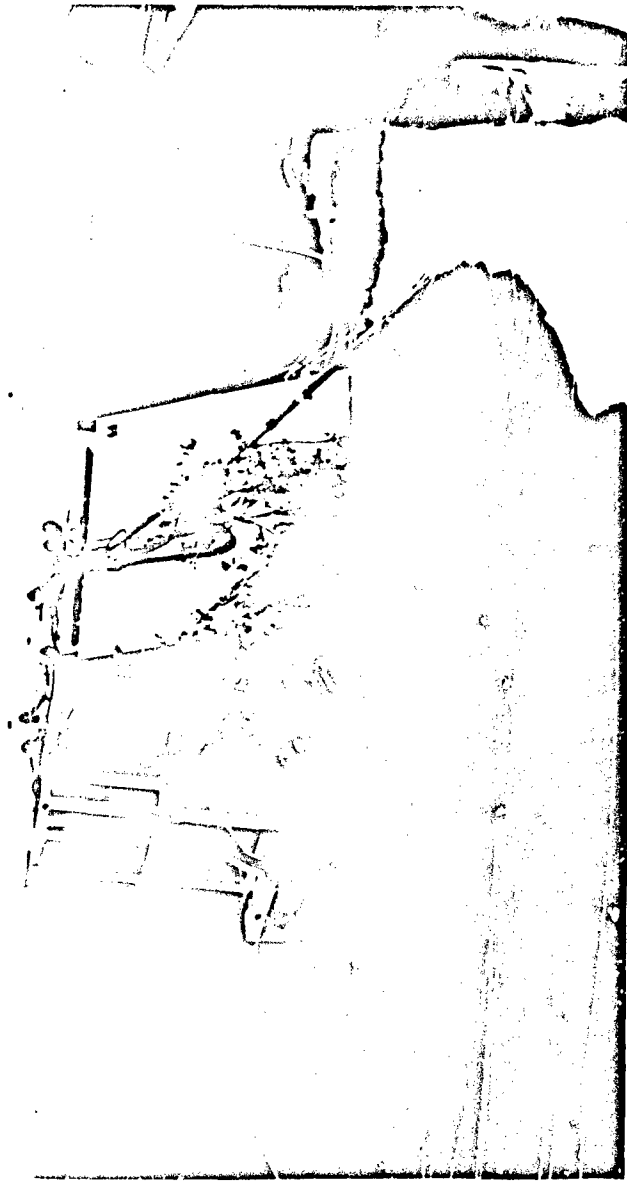


Figure 24. ABLE Payload at Recovery Site

A computer system, developed by Physical Science Labs, was used to output lidar data graphically during the flight. A typical quick-look plot of lidar data is shown in Figure 25. Because of a software error in the PSL computer system, no GRN detector data were displayed in real time. Post flight analysis has demonstrated that the detector operated properly and that the two color lidar data was received.

8. RECOMMENDATIONS AND CONCLUSIONS

Visidyne, Inc, recommends the following tasks be performed prior to any future ABLE flight:

8.1 Frame

Perform a general inspection with overall examination of structural integrity of payload framework to insure all damaged or distorted elements are replaced and/or repaired. Restore all optics to preflight specifications, including recoating of optical surfaces, if required. Replace the laser mirror. Check and confirm the integrity of all electronic circuitry including connectors and cable runs.

8.2 Laser Refurbishment

Clean, test, and recalibrate the laser system; replace flashlamps and provide optical and alignment checks, and verify that laser system has been restored to original preflight condition. Add an alignment laser.

8.3 Harmonic Generator Encoder

Replace present motor micrometers with digital-indicating motor micrometers, and incorporate into telemetry a status indication of the laser tuning.

8.4 Thermal Control System Modification

Perform an evaluation and redesign of the lidar thermal control system to provide the thermal environment required for proper inflight operation. Local validation testing of designed system components shall be done if it can be performed at a reasonable cost.

8.5 Laser Signal Detector

Upgrade and improve the laser beam energy monitor to reduce the noise environment, and increase the signal-to-noise level at all laser emitted wavelengths. Make operational the detector aliveness checkout system.

8.6 1064 nm Detector

Incorporate a 1064 nm wavelength detector system.

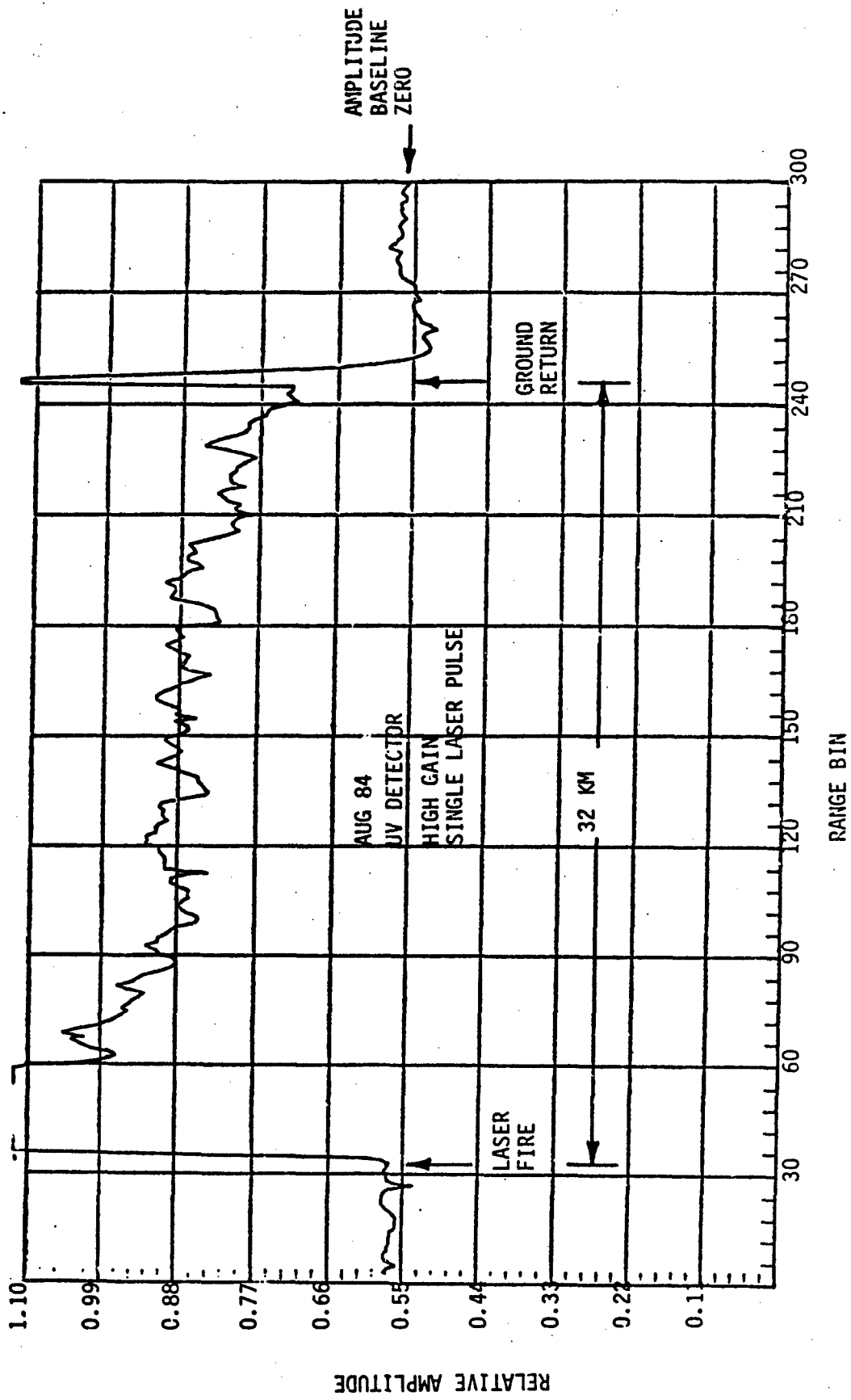


Figure 25. ABL Quick-Look Lidar Data

8.7 Summary

The development and flight test of the ABLE payload was successful, and all technical objectives were achieved. It is recommended that the acquired data be analyzed, and the payload be refurbished, upgraded, and flown again.

THIS PAGE LEFT BLANK INTENTIONALLY

9. REFERENCES

1. Brehm, W.F., and J.L. Buckley, "Design Study of a Laser Radar System for Spaceflight Application", G.E. SpaceDivision, AFG-TR-79-0264 (Dec. 1979), ADA082332.
2. Shepherd, O., G. Aurilio, R.D. Bucknam, R.W. Brooke, A.G. Hurd, and T.F. Zehnpfennig, "Balloonborne Lidar Experiment", Visidyne, Inc., AFGL-TR-80-0373 (Dec. 1980), ADA095366.
3. Yoder, P.R., Jr., F.B. Patrick, and A.E. Gee, J. Opt. Soc. Am., 43, 1200 (1953).
4. Gascoigne, S.C.B., Appl. Opt., 12, 1419 (1973).
5. "American National Standard for the Safe Use of Lasers", ANSI Z136.1-1980 American National Standards Institute, Inc., New York, NY (1980).

THIS PAGE LEFT BLANK INTENTIONALLY

REPORT ON LIDAR BALLOON GONDOLA FRAME ANALYSIS

The Gondola Frame for the Lidar Balloon Experiment was analyzed for the following conditions: Launch, Float Operational, Parachute Deployment and Survival Crash. The program used for all the analyses was ADINA (Automatic Dynamic Incremental Nonlinear Analysis), a proprietary code developed by Prof. K.J. Bathe, Department of Mechanical Engineering, MIT, and first released in 1975. The program can be used for linear and non-linear, static or dynamic analysis of structures. The following elements are included in the element library: A 3-D truss, a 3-D beam, a plane-stress, plane-strain or axisymmetric isoparametric element with 4 to 8 nodes, a 3-D isoparametric solid or thick shell element with 8 to 21 nodes, a general thin-shell or thin plate element with 3 to 16 nodes, and 2-D or 3-D fluid elements. The program consists of more than 40,000 source statements. It is believed to be the most efficient general purpose code available, especially for linear analysis.

Three cases were considered for the Float operational conditions: 1°C Temperature differential between top and bottom, 1°C Temperature differential between left and right side and 1 g vertical acceleration (gravity). The two temperature gradient analyses used 216 3-D beam elements and 87 nodes. The nodes coincided with those actually present in the three-dimensional frame. For the 1-g analysis, 19 intermediate nodes were introduced along the members which carried the instruments, etc., and the number of beam elements increased to 235. For the float operational condition, the result of interest is the misalignment between the axes of the transmitter and the receiver. It was found that the 1.0g gravity load will change the angle between the axes of these instruments by 0.0014° . This relative rotation between the axes will be almost exclusively in a vertical plane. The change in angle produced by a 1°C difference

between the left and right sides is 0.0008° and occurs mostly in the horizontal plane. Finally, the change in angle caused by 1°C vertical gradient is 0.0018° and is almost entirely in a vertical plane.

The launch condition of 2.0g vertical acceleration causes internal forces and relative displacements which are twice those computed for the 1.0g vertical acceleration. These forces and deformations are well within the elastic range, and therefore produce no permanent distortions.

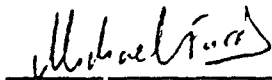
For parachute deployment, it was assumed that the entire weight of the gondola (excluding the 600 lb ballast) is taken by one cable and one eyebolt alone, and that the gondola rotates so that its center of gravity lies directly underneath this latter eyebolt. The gondola was assumed to be subjected to a constant vertical acceleration of 10 g. Computed internal forces were within the elastic range of the material: The most severely stressed member was the vertical angle directly underneath the eyebolt that takes the entire load. This member had an axial tension of 9954 lb and a maximum moment of 618 lb in. These forces result in a maximum tensile stress of 16,900 psi. The maximum stress in the tubular members of the middle deck was only 1,800 psi.

In the crash analysis it was assumed that the gondola lands on the corner nearest to the receiver-detector. The direction of the frame upon landing was assumed such that the center of gravity falls directly above the corner in question. This corresponds to a rotation of the frame in a vertical plane by 72° . The acceleration at landing was assumed equal to 10g. The computed internal forces at the middle deck were within the elastic range: The maximum stress in the biaxially bended tubular members there was only 4,100psi. The members of the bottom deck near the corner of impact were found to be severely overstressed: The maximum compressive force was found in one of the two 24-in-long horizontal

angles leading to the corner: 8513 lbs. The corresponding biaxial moments M_x and M_y are 1625 lb in and 216 lb in. These internal forces produce a maximum compressive stress of 21,600 psi. (The member has a slenderness ratio of 39.2 and its elastic buckling stress is 64,200 psi, higher than its yield stress.) The maximum compressive stress at the bottom deck occurs at one of the two 31.25-in-long horizontal sides of the cubical frame passing through the corner of impact. This member has a compressive force of 6142 lb (corresponding stress: 8,530 psi, less than the critical elastic buckling stress of 37,900 psi) and moments M_x , M_y of 5,097 lb in and 2,277 lb in. The resulting maximum compressive stress of 47,600 psi exceeds the material strength.

Overall, the frame was found to be stiff enough to retain alignment of the instruments during operation, and strong enough to survive the postulated parachute deployment and crash conditions with only minor damage in some of the members that do not support directly any important instruments.

Signed by:

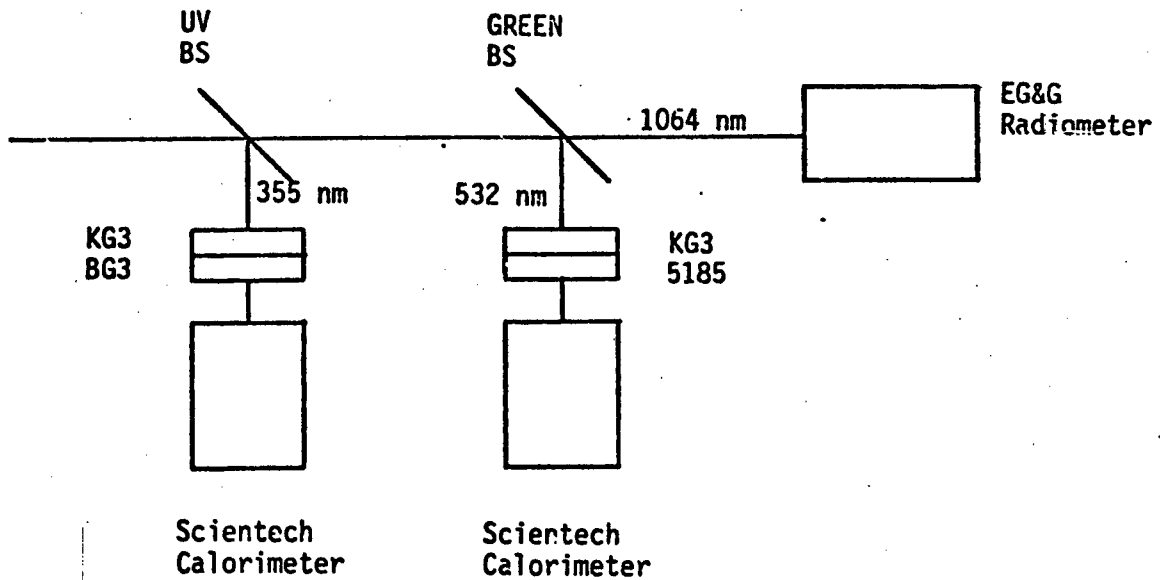


Date: Jan. 11, 1982

Michael N. Fardis, Ph.D.
302 LaGrange Str.
Newton, MA 02167

THIS PAGE LEFT BLANK INTENTIONALLY

ABLE LASER TEST SUMMARY



Standard Laser Calibration

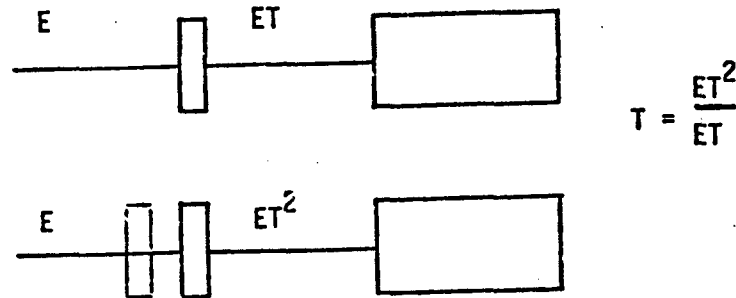
Standard Procedures

- a. Tune GREEN SHG for maximum GREEN output
- b. Tune UV THG for maximum UV output
- c. Maximize UV output by detuning GREEN SHG

Wavelength	Single Wavelength		Estimated Internal Max. Energy/Pulse
	Maximum Energy/Pulse	Nominal Energy/Pulse	
1064 nm	434 mJ	220 mJ	538 mJ
532 nm	150 mJ	76 mJ	161 mJ
355 nm	44 mJ	38 mJ	44 mJ

Tests

- a. Compared EG&G radiometer calibration to Scientech at 1064 nm.
- b. Measured UV and GREEN filter transmission by inserting a second filter in the beam and ratioing the measured transmitted energy.



	532 nm	KG3 BG3 355 nm (AFGL Filter)
Filter Transmission	0.369	=0.716

- c. Measured beam splitter losses: GREEN energy transmission of UV Beam splitter = 0.94, RED energy transmission of UV Beam splitter = 0.92, RED energy transmission of GREEN Beam splitter = 0.88.
- d. Confirmed that the beam splitter transmission and reflection were independent of the polarization of the incident energy and independent to small changes in the angle of incidence.
- e. Confirmed that the energy/pulse at all three wavelengths was stable with time after a several minute warmup period.

APPENDIX C

PRE-FLIGHT BRIEFING/ABLE

20 AUG 1984

PRE-FLIGHT BRIEFING		
L. BRIEFING DATE/TIME 20 Aug 84/1300L		FLIGHT NUMBER H84-2?
I. GENERAL DATA		
1. PROJECT NO. & TITLE 76701511/ABLE		5. PROJECT OFFICER Mr. Griffin
2. EXPERIMENTER AFGL/Visidyne	4. FLIGHT OBJECTIVES A. Float at approx 100k MSL across NSMR and acquire atmospheric density data with LIDAR	
3. REQUIRED FLIGHT PROFILE Climb to float; Float across NSMR; Terminate		6. TEST COORDINATOR N/A
7. LAUNCH CREW CHIEF SSgt Darden	8. MISSION CODE	9. SCHEDULED LAUNCH A. MYS Roswell IAC, NM B. DATE/TIME 21 Aug 84/2000L
10. TERMINATION DATE/TIME 22 Aug 84/0015L	11. PAYLOAD 2700 lbs 2700 lbs	12. FREE LIFT 12K
II. BALLOON DATA		
1. BALLOON NO. 1 OF 1 ITEM N/A S/N 0008 CONTRACT SE277.88-100-NSC-01 M42476		
2. MANUFACTURER Winzer	3. DIAMETER (ft) 277.83 ft	
4. LENGTH (ft) 108.91 ft	5. VOLUME (ft ³) 8.74 x 10 ⁶ ft ³	
6. WEIGHT (lb) 2403 lbs	7. MATERIAL & THICKNESS Strotofilm/1.0 mil/2-1.0 mil caps	
8. MODEL NO. (SI) SV-008	9. VALVE & VALVE MOTOR S/N EV-13/BX0117/Motor # 1046	
10. BALLOON DESTRUCT Dual Rip Lines	11. REFLECTIVE TAPES Yes	
III. PARACHUTE DATA		
1. SERIAL NO. (SI)/MFR DATE 598574		
2. QUANTITY/TYPE/DIAMETER (SI)/WEIGHT (SI) 1 ea/Flat circular/100 ft Diameter/187 lbs		
3. LENGTH (ft) 150 ft	4. BURST SWITCH <input checked="" type="checkbox"/> YES <input type="checkbox"/> NO	5. PLANNED DESCENT LOAD 2000 lbs 2120
IV. INSTRUMENTATION DATA		
1. PACKAGE TYPE PCNII	2. ALTITUDE SENSORS (TYPE, S/N) CIC 0-15; 0-2; 0-0.2 PSI	
3. ANTENNA DEPLOY ANEROID ALT. N/A	4. BURST/IMPACT SWITCH ARM ALT. 10 k MSL/Command	
5. RADIOCODE <input type="checkbox"/> STANDARD N/A <input type="checkbox"/> EXTENDER <input type="checkbox"/> OVERSOUND		
FREQUENCIES: COORDINATION WITH SET 1/SET 2 DATE/TIME N/A		
6. COMMAND RECEIVER A. PRIMARY (SI) 437.5 MHz B. BACK-UP 437.5 MHz		7. TRANSMITTER A. PRIMARY 2258.5 MHz B. BACK-UP 2258.5 MHz
8. TRANSMITTER ANTENNA LENGTH A. PRIMARY N/A B. BACK-UP N/A		
9. PRIMARY COMMANDS ARE: IIR/SEQUENCES, CHANNELS & FUNCTIONS See Technical Data		
CH 1	CH 2	CH 3
CH 2	CH 3	CH 4
CH 3	CH 4	CH 5
10. BACK-UP COMMANDS ARE (IIR) SEQUENCES, CHANNELS & FUNCTIONS See Technical Data		
CH 1	CH 2	CH 3

AFGL FORM 89

PREVIOUS EDITION WILL BE USED

AFSC - MANCOM AFS MA 700

11. DROPPABLE BALLAST			
A. TYPE <u>GLASS</u>		B. WEIGHT <u>600 lbs</u>	C. HOPPERS <u>2</u>
D. 'BLOW' VCS	E. SLUGS <u>N/A</u>	F. TOTAL FLOW RATE <u>64 LB/HR</u>	G. DRIFTS MIS <u>None</u>
12. SAFETY TIMER <u>N/A</u> MINUTES BELOW <u>KPT</u>			
13. TERMINATION TIMERS: A. PRIMARY <u>8.0 hrs</u> B. SECONDARY <u>N/A</u>			
14. IMPACT SWITCHES <u>4 ea/AFGL</u>		A. ARM ALTITUDE <u>10k NSL</u>	
15. RADAR REFLECTORS <u>None</u>		16. FLASHING LIGHT LOCATIONS <u>BTZF & Payload</u>	
V. VOICE COMMUNICATIONS DATA			
1. FREQUENCIES:			
A. HF (1) <u>11175 (B)</u> (B) (B)		B. VHF (1) <u>138.875 MHz</u>	
<u>138.875 MHz</u>		C. UHF (1) <u>None</u> (B) (B)	
(B) 141.8 MHz		D. SPECIAL <u>None</u>	
2. CALL SIGNS:			
A. CONTROL CENTER <u>Roswell Control</u>		B. VAN <u>FH TM</u>	
C. RECOVERY <u>FH 11/FH 1A</u>		D. AIRCRAFT <u>FH 60</u>	
VI. REPORTING TIMES			
1. LAUNCH PERSONNEL AT SLOC <u>Roswell</u>		2. CONTROL CENTER OPEN <u>1530L</u>	
<u>1670</u> AT <u>1530L</u>		<u>1530L</u>	
3. REMOTE RENDEZVOUS: A. TIME <u>N/A</u> B. PLACE			
VII. AIRCRAFT SUPPORT			
1. A. TYPE <u>Cessna 206</u>		B. TAIL NO. <u>N35877</u>	
C. TAKE-OFF TIME <u>22/0600</u>			
2. A. TYPE <u>UH-1 (Army)</u>		B. TAIL NO. <u>Unkn</u>	
C. TAKE-OFF TIME <u>22/TRD</u>			
VIII. LAUNCH DATE SUPPORT			
1. METEOROLOGY <u>Pibals</u>		2. COC PHOTO/VIDEO <u>Still & Video</u>	
3. OTHER <u>None</u>			
IX. RANGE SUPPORT			
1. RADAR A. TRACKING AOS TO LOS		B. TRANSPONDER AOS TO LOS	
C. DENTAL AOS TO LOS		2. OPTICS <u>N/A</u> TO	
3. OTHER <u>None</u>			
X. TRACKING SUPPORT			
1. THEODOLITE <input checked="" type="checkbox"/> YES <input type="checkbox"/> NO		2. PRA <input checked="" type="checkbox"/> YES <input type="checkbox"/> NO	
3. GND <input type="checkbox"/> YES <input type="checkbox"/> NO		4. RADAR <input checked="" type="checkbox"/> YES <input type="checkbox"/> NO	
5. VOR <input type="checkbox"/> YES <input type="checkbox"/> NO		6. AIRCRAFT <input checked="" type="checkbox"/> YES <input type="checkbox"/> NO	
7. OTHER <u>N/A</u>			
XI. SPECIAL TEST REQUIREMENT/EQUIPMENT			
1. <u>SPY W/TIAS at Bldg 850 for TM & Backup Tape Recording</u>			
XII. REMARKS			
<u>None</u>			

APPENDIX D

FLIGHT CONTROL PERSONNEL AND WORK STATION

DSGN.	NAME/ORG.	RESPONSIBILITY/WORK STATION
FH2/FTD	A. GRIFFIN/AFGL	AFGL PROJECT OFFICER/FLIGHT LINE/CC VAN, ROSWELL
	W. KEIFER/AFGL	AFGL PROJECT OFFICER/BLDG. 850, HAFB
FHTM	R. LAVIGNE/AFGL	BALLOON CONTROL & TM/TM VAN, ROSWELL
FHC	J. JACOBY/AFGL	BALLOON FLIGHT CONTROL/CC VAN, ROSWELL
FH-4	S/SGT DARDEN	LAUNCH CREW CHIEF/FLIGHT LINE
PM	D. BEDO/AFGL	PROGRAM MANAGER/BLDG. 850, HAFB
TPM	R. SWIRBALUS/AFGL	TECHNICAL PROGRAM MANAGER/FLIGHT LINE/TM VAN, ROSWELL
TC	J. HUGHES/AFGL	TEST CONDUCTOR/TM VAN ROSWELL
VI-1	O. SHEPHERD	VISIDYNE PROJECT OFFICER/FLIGHT LINE/BLDG 850, HAFB
VI-2	R. BUCKNAM	VISIDYNE ALT. PROJECT OFFICER/FLIGHT LINE
VI-3	A. HURD	ABLE COMMAND OFFICER/BLDG. 850, HAFB
VI-4	W. SHEEHAN	ALT. TEST CONDUCTOR/TM VAN, ROSWELL
PSL-1	R. BRAMLETT	COMPUTER CONTROL/BLDG. 850, HAFB

THIS PAGE LEFT BLANK INTENTIONALLY

APPENDIX E

LAUNCH SCHEDULE

(10)	L-3days	Launch Simulation
(20)	L-6hrs	Final External Check
(30)	L-4hrs	Report
(40)	L-3½hrs	Rollout
(50)	L-3hrs	Start Internal Checks
(60)	L-2½hrs	Internal Power Payload Check
(70)	L-2hrs	Balloon Layout
(80)	L-1½hrs	Payload Switches Set
(90)	L-1hr	Begin Inflation
(100)	L-15min	Payload Power Launch Config.
(110)	L-0	Launch

THIS PAGE LEFT BLANK INTENTIONALLY

APPENDIX F

PROJECT ABLE

LAUNCH COUNTDOWN

AUGUST 1984

<u>L. MINUS TIME (HRS)</u>	<u>LOCAL TIME</u>	<u>EVENT</u>
L. - 34		ALL SYSTEMS CHECK
L. - 5	1500	WEATHER BRIEFING
L. - 4½	1530	PERSONNEL REPORT TRANSFER PAYLOAD TO CRANE
L. - 4	1600	MOVE TO LAUNCH SITE
L. - 3½	1630	COMMENCE ALL INSTRUMENT CHECKS
L. - 2¾	1745	INSTRUMENT CHECKS COMPLETE FINAL WEATHER UPDATE (GO/NOGO)
L. - 2	1800	BALLOON LAYOUT
L. - 1½	1845	RIG ALL BALLOON SYSTEMS HOT VALVE CHECK PAYLOAD READIED FOR LAUNCH
L. - 1	1900	BEGIN INFLATION
L. - 15min	1945	SET PAYLOAD TO LAUNCH CONDITION
L. - 10 min	1950	PERMISSION TO LAUNCH
L. - 0	2000	LAUNCH

THIS PAGE LEFT BLANK INTENTIONALLY

INSTRUMENTATION CHECKS

Tone Commands	FUNCTION	VERIFY
207	RCVR POWER - ON	VALID PCM LOCK
213	THERMAL CONTROL POWER - ON	Page 2 THERM CONT VMON
210	SECONDARY COOLANT PUMP - ON	Page 4 SEC. PUMP FLOW
201	LASER POWER - ON	(Headings any page)
209	COMPUTER BOOT	5 SEC MODULATION LOS.
Modem Commands		
	<u>POINTING MIRROR TEST</u>	
ACREQ PU	POINTING MIRROR UP	Page 5
ACREQ PD	POINTING MIRROR DOWN	Page 5
ACREQ PH	POINTING MIRROR HORIZONTAL	Page 5
	<u>HARMONIC GENERATOR TEST</u>	
ACREQ HGDWVG	UV UP DOWN MED. SPEED CLOCK - GO	Page 5
S	STOP	Page 5
J	JOG	Page 5
X	EXIT	
	<u>DETECTOR POWER</u>	
ACREQ DI	BOTH DETECTORS - ON	Page
Tone Commands		
203	LASER ARM	Headings any page
201 HOLD	LASER FIRE (<u>Hold Command</u>) !	Headings any page

L - 3½ hrs. START INSTRUMENTATION CHECK (1630)

Modem
Commands

Function

Verify

FIRING RATES

ACREQ L2	LASER FIRING RATE = 5pps	Page 5
ACREQ L1	LASER FIRING RATE = 2.5pps	Page 5
ACREQ L0	LASER FIRING RATE = 1.25pps	Page 5
ACREQ L3	LASER FIRING RATE = 10pps	Page 5

Tone
Commands

205 (<u>Open</u>)	LASER FIRE OFF	(Heading any page)
204	LASER SAFE	(Heading any page)

Modem
Commands

DETECTOR POWER

ACREQ D0	BOTH DETECTORS - OFF	Page 5
----------	----------------------	--------

POINTING MIRROR

ACREQ PS	POINTING MIRROR STOW	Page 5
----------	----------------------	--------

tone
Commands

202	LASER POWER OFF	(Heading any page)
211	SECONDARY COOLANT PUMP OFF	Page 5
214	THERMAL CONTROL POWER OFF	Page 5
208	RECEIVER POWER OFF	Page 5

APPENDIX H

PRE-FLIGHT CHECK LIST

T - 1hr 15 min (1845) PAYLOAD FLIGHT CONFIGURATION

1. TELESCOPE COVER - OFF
2. POINTING MIRROR COVER - OFF
3. LASER UP AND DOWN BAFFLE COVERS - OFF
REMOVE HORIZONTAL LASER DUMP
VISUAL INSPECTION OF LASER POINTING MIRRORS
INSTALL HORIZONTAL LASER DUMP
4. POWER DISTRIBUTION
HOUSEKEEPING POWER SWITCH ON
(BAT UP)
5. THERMAL CONTROL POWER SWITCH ON
(BAT UP)
6. STATUS IND SWITCH - OFF
7. ARM KEY - INSTALLED - ARM SWITCH IN ARM POSITION
8. FIRE KEY - INSTALLED - FIRE SWITCH IN FIRE POSITION

THIS PAGE LEFT BLANK INTENTIONALLY

APPENDIX I

PRE-ROLLOUT CHECK

1. FOUR BATTERY BOXES CONNECTED PLUS SWITCH CONNECTOR ON THERMAL CONTROL BATTERY BOX
2. ALL BATTERY BOX FUSES, BUSSED
3. DIODE PLATE FUSES, BUSSED
4. MOTOR DRIVE CONNECTOR, CONNECTED
5. TEMPERATURE SENSOR CONNECTORS (4)
6. ALL FLUID LINES CONNECTED
7. CRUSH PADS INSTALLED
8. THERMAL CONTROL SWITCH - UP POSITION
9. HOUSEKEEPING SWITCH - UP POSITION
10. GSE CONNECTOR (P201) OUT (P49) OUT AND REMOVE T/M CABLE PLUGGED INTO P201
11. IND. SWITCH - ON POSITION
12. VISUAL INSPECTION OF PAYLOAD
13. CLEAN PAYLOAD
14. BAG PAYLOAD

THIS PAGE LEFT BLANK INTENTIONALLY

ABLE FLIGHT CONDITIONS

*NOTE - - ALL LASER FIRING MUST BE APPROVED BY D. BEDO AT BLDG. 850

PROCEDURES TO KEEP TEMPERATURE OF PRIMARY COOLANT RESERVOIR $> 0^{\circ}\text{C}$ AND LESS THEN 35°C
(Cont'd)

- b) AT ANY ALTITUDE, TURN OFF SECONDARY COOLANT SYSTEM
- c) WHEN PRIMARY COOLANT RESERVOIR TEMPERATURE IS GREATER THAN 15°C , STOP LASER FIRING AND/OR START SECONDARY COOLANT SYSTEM

ALTITUDE \approx 20K FT. CONFIRM "ALT: AT ALT" Page 5

IF "NOT AT ALT" AT 25K FT., THE INTERLOCK OVERRIDE COMMAND MUST BE SENT IF HEAT IS TO BE GENERATED IN THE PRIMARY SYSTEM

ALTITUDE 60K FT.

POINTING MIRROR UP

DETECTORS ON

LASER ARM

*LASER FIRE

PER D. BEDO

OVER RANGE

LASER SAFE

POINTING MIRROR - DOWN

LASER ARM

*LASER FIRE

IF TEMPERATURE OF RAD 1 OR RAD 2 IS GREATER THAN -35°C AND LASER PRIMARY COOLANT TEMPERATURE IS LESS THAN 0°C - TURN OFF SECONDARY COOLANT PUMP

IF TEMPERATURE OF PRIMARY COOLANT RESERVOIR IS GREATER THAN 35°C AND SECONDARY COOLANT PUMP IS ON, INTERRUPT FIRING

EMERGENCY SHUT DOWN PROCEDURE

202

LASER POWER OFF

214

THERMAL CONTROL POWER OFF

208

RECEIVER POWER OFF